1-1-2013

Detection of Thermoluminescence in Polyether Ether Ketone (PEEK)

Dipendra Adhikari

DETECTION OF THERMOLUMINESCENCE IN POLYETHER ETHER KETONE (PEEK)

by

Dipendra Adhikari

A Thesis

Submitted in Partial Fulfillment of the

Requirements for the Degree of

Master of Science

Major: Physics

The University of Memphis

December 2013

ACKNOWLEDGEMENTS

I would like to thank Dr. M. S. Jahan for his continuous guidance, enormous help and support throughout this work. I am indebted to him for his patience, unending commitment for this work and insightful suggestions. I am heartily grateful to Dr. Hai Trieu for his valuable suggestions and encouragements throughout the work.

I would like to show my appreciation to Dr. Sanjay R. Mishra and Dr. John W. Hanneken for taking their valuable time to participate as a member of my thesis committee and for their valuable suggestions and comments after reading the final draft of my thesis.

My special thanks go to coworkers Benjamin M. Walters, R. Gnawali, and T. Riahinasab for supporting me in my entire research time.

I am grateful to all of my professors and friends in the Department of Physics and The University of Memphis, for giving me this opportunity.

I am indebted to my parents, relatives, and friends for their inspiration for me to pursue my higher study. Finally, I would like to thank my wife, Binita Tripathi Adhikari, for her inspiration, love, and mental support without which it would be quite difficult to finish this work.

ABSTRACT

Adhikari, Dipendra. MS. The University of Memphis, December 2013. Detection of Thermoluminescence in Polyether ether ketone (PEEK). Major Professor: M. Shah Jahan, PhD.

Sterilization is a mandatory process for materials used in medical applications. Sterilization procedures commonly used are steam sterilization, ethylene oxide (EtO) sterilization and sterilization by radiation. The high energy photons incident upon a polymer can cause chain scission, crosslinking, defects (trapped electrons) within the polymer matrix, and the formation of free radicals.

In this research work, we used thermally stimulated luminescence (TSL) and differential scanning calorimeter (DSC) to study the effects of X- and UV-irradiation on different grades of PEEK. We have observed a major sharp glow peak at temperature of about 150°C (with other five minor peaks), at the glass transition temperature of PEEK, similar to previous researchers. After X- and UV- irradiation the peak at about 100°C is much more affected by radiation. Initially, its intensity increases rapidly with the time of exposure to radiation and then increases slowly. Also, the observation showed that, after irradiation the intensity of peak at 100ºC decreases rapidly as the time passes and the effect of radiation persists for only about 24 hours after irradiation. The PEEK polymer is affected more by X-ray in comparison with UV-radiation. TSL of preheated samples of PEEK shows glow peak at about 75ºC and its intensity is found to increase with increase in preheat temperature. Moreover, the initial major TSL peak at about 150ºC completely disappear when the PEEK (film) is preheated at 250ºC for one hour in air and it reappears again as the sample is stored for longer time (within one day) at room temperature.

DSC measurement shows a large exothermic crystallization peak at temperature 180℃ for PEEK film. This indicates that material has a strong tendency to crystallize. We observed that the glass transition temperature (T_g) increases and melting temperature (T_m) decreases slightly as a result of X-irradiation for all types of PEEK. Similar observations were made by past researcher in PEEK for γ- and e-beam irradiation. The shift of T_g to higher temperature and T_m to lower temperature with irradiation suggest that both cross-linking as well as chain scission mechanisms take place due to X-irradiation.

TABLE OF CONTENTS

	PAGE
CHAPTER 1. Introduction	1
1.1 Polymer	1
1.2 Biomaterials	2
1.3 Polymeric biomaterials	3
1.4 Polyether ether ketone (PEEK)	5
1.5 Different grades of PEEK	9
1.6 Background	11
1.6.1 Unfilled PEEK	11
1.6.2 CFR-PEEK	14
1.7 Motivation for present study	17
CHAPTER 2. Theory	19
2.1 Thermoluminescence or thermally stimulated luminescence (TSL)	19
2.2 Thermoluminescence models	20
2.2.1 Jablonski model	21
2.2.2 Configurational-coordinate model	22
2.2.3 Energy band model	23
2.3 Order of kinetics	24
2.3.1 First order kinetics (slow retrapping)	24
2.3.2 Second order kinetics (fast retrapping)	24
2.4 Thermoluminescence in polymers	27

2.4.1 Eletron traps and luminescence centers 27

2.5 Differential scanning calorimetry (DSC) 28

CHAPTER 3. Materials and method 31

3.1 TSL measurement 31

3.2 DSC measurement 32

3.3 Groups of PEEK samples 34

CHAPTER 4. Results and discussion 37

4.1 TSL analysis of X- and UV-irradiated PEEK 37

4.1.1 TSL in PEEK film 37

4.1.2 TSL in CFR-PEEK 49

4.1.3 TSL in HT-PEEK 50

4.1.4 TSL in unfilled PEEK (rod) 51

4.1.5 TSL in preheated samples of PEEK 51

4.2 DSC measurements 56

4.2.1 DSC of X-irradiated PEEKs 56

4.2.2 DSC of preheated samples of PEEK film 59

4.3 Conclusion and future work 60

References 61

Appendix 65

LIST OF TABLES

Table Page

1-1: Comparison of some physical properties of different grades of PEEK 10

4-1: Observed values of T_g, T_c and T_m for different PEEK 58

4-2: Observed values of T_g, T_c and T_m for PEEK film preheated at 250°C in air for 1 hour 59

A-1: TSL parameter for non-irradiated PEEK film 65

A-2: TSL parameters for PEEK film X-irradiated for 10 minutes 65

a) Immediately after irradiation 65

b) 15 minutes after irradiation 65

c) 25 minutes after irradiation 66

d) 48 hours after irradiation 66

A-3: TSL parameters for PEEK film X-irradiated for 20 minutes 66

a) Immediately after irradiation 66

b) 15 minutes after irradiation 67

c) 25 minutes after irradiation 67

d) 1 hour after irradiation 67

A-4: TSL parameter for PEEK film X-irradiated for 30 minutes 68

a) Immediately after irradiation 68

b) 15 minutes after irradiation 68

c) 51 minutes after irradiation 68

d) 1 hour and 27 minutes after irradiation 69

A-5: TSL parameter for PEEK film X-irradiated for 40 minutes 69

a) Immediately after irradiation 69

b) 15 minutes after irradiation 69

c) 30 minutes after irradiation 70

d) 1 hour after irradiation 70

A-6: TSL parameter for PEEK film X-irradiated for 50 minutes 70

a) Immediately after irradiation 70

b) 15 minutes after irradiation 71

c) 45 minutes after irradiation 71

d) 24 hours after irradiation 71

A-7: PEEK film X-irradiated for 60 minutes 72

a) Immediately after irradiation 72

b) 15 minutes after irradiation 72

c) 33 minutes after irradiation 72

d) 1 hour after irradiation 73

e) 24 hours after irradiation 73

A-8: Area under a peak for x-irradiated samples of PEEK film immediately after irradiation for different time 73

A-9: Area under a peak for x-irradiated samples of PEEK film 74

a) X-irradiated for 10 minutes 74

b) X-irradiated for 20 minutes 74

c) X-irradiated for 30 minutes 74

d) X-irradiated for 40 minutes 75

e) X-irradiated for 50 minutes 75

f) X-irradiated for 60 minutes 75

Table A-10: Area under a peak for PEEK film preheated in air

for 1 hour at 250ºC 76

LIST OF FIGURES

Figure	Page
1-1. Chemical structure of PEEK	5
1-2. Structure of	
(A) Chain conformation of PEEK	7
(B) Crystal structure of PEEK	7
2-1. A typical TSL glow curve	20
2-2. Jablonski's model for	
(A) Fluorescence	21
(B) Phosphorescence	21
2-3. Configurational Coordinate Diagram	22
2-4. A schematic representation of a simple energy-band model in solids	23
2-5. A typical DSC heating curve	28
3-1. TSL experimental setup (Harshaw QS 3500)	32
3-2. A block diagram of TSL reader	32
3-3. Schematic diagram of Differential Scanning Calorimeter	33
4-1. TSL glow curve for non-irradiated PEEK film	37
4-2. TSL glow curves for 10 minutes X-irradiated PEEK film	38
4-3. TSL glow curves for 20minutes X-irradiated PEEK film	39
4-4. TSL glow curves for 30 minutes X-irradiated PEEK film	40
4-5. TSL glow curves for 40 minutes X-irradiated PEEK film	41
4-6. TSL glow curves for 50 minutes X-irradiated PEEK film	42
4-7. TSL glow curves for 60 minutes X-irradiated PEEK film	43-44

4-8. Combined TSL glow curves for PEEK (film) for different X-irradiation time 45

4-9. Growth of peak 2 and 4 with time of X-ray exposure 45

4-10. Line graph for decay behavior for peak 2 and 4 for X-irradiated PEEK film 46

4-11. TSL glow curve for UV-irradiated PEEK film 47

4-12. Glow curves for X- and UV-irradiated CFR-PEEK 49

4-13. TSL in X- and UV-irradiated HT-PEEK 50

4-14. TSL in X- and UV-irradiated plain PEEK (rod) 51

4-15. Glow curves for preheated PEEK film 52

4-16. Glow curves for 1 hour preheated samples of PEEK film at 250°C in air 52

4-17. Deconvoluted glow curves for 1 hour preheated PEEK film at 250°C in air 53

4-18. Line graph showing decay of Peak 2 and growth of peak 4 for 1 hour preheated PEEK film at 250°C in air 54

4-19. TSL glow curves for preheated CFR-PEEK 54

4-20. TSL glow curves for preheated sample of HT-PEEK 55

4-21. TSL glow curves for preheated sample of Unfilled PEEK (rod) 55

4-22. DSC heating curves of PEEK film 56

4-23. DSC heating curves of CFR-PEEK 57

4-24. DSC heating curves of HT-PEEK 57

4-25. DSC heating curves for

a) Preheated PEEK film for 1 hour at 250°C in air 59

b) DSC curves for PEEK film for first and second run 59

CHAPTER 1

Introduction

1.1 Polymer

We live in a polymer age. Plastics, fibers, elastomers, coatings, adhesives, rubber, protein, cellulose etc., are all common terms in our modern vocabulary, and all a part of the fascinating world of polymer science. Polymers have extraordinary range of properties and they have wide range of application in our everyday life. On the basis of their origin, there are two types of polymers [1, 2]:

- Natural polymers
- Synthetic polymers

Natural polymers occur in nature and they can be extracted. Silk, Wool, DNA, Cellulose, Proteins etc. are some examples of commonly used natural polymers. Synthetic polymers are derived from petroleum oil and are man-made polymers. Examples of some synthetic polymers are Nylon, Polyethylene, Polyester, Teflon, Epoxy etc. [3]. Many Scientists had important contribution to improve the properties of polymers for specific applications. Now a days, we have seen a number of important advances in polymer science as [4]:

- Engineering plastics-polymers designed to replace metals.
- Polymers having excellent thermal and oxidative stability for use in high performance aerospace applications.
- Nonflammable polymers, including some that emit a minimum of smoke or toxic fumes.
- Polymers for a broad spectrum of medical applications.

- Degradable polymers, which not only help to reduce the volume of unsightly plastics waste but also allow controlled release of drugs or agricultural chemicals.
- Conducting polymers-polymers that exhibit electrical conductivities comparable to those of metals.

1.2 Biomaterials

Biomaterials are materials intended to interface with biological systems to evaluate, treat, augment, or replace any tissue, organ, or function of the body. The essential property of a material to accept as a biomaterial is it should be biocompatible. The ability of a material to perform with an appropriate host response in a specific application is called biocompatibility [5].

Polymers form a versatile class of biomaterials that have been investigated for medical and related applications [2]. This can be attributed to the inherent flexibility in synthesizing or modifying polymers matching the physical and mechanical properties of various tissues or organs of the body. The development of polymeric biomaterials can be considered as evolutionary process. Reports on the applications of natural polymers as biomaterials date back thousands of years [6]. However, the application of synthetic polymers to medicine is more or less a recent phenomenon.

Medical practice today utilizes a large number of devices and implants. Biomaterials in the form of implants (sutures, bone plates, joint replacements, ligaments, vascular grafts, heart valves, intraocular lenses, dental implants, etc.) and medical devices (pacemakers, biosensors, artificial hearts, blood tubes, etc.) are widely used to replace and/or restore the function of traumatized or degenerated tissues or organs, to assist in

healing, to improve function, to correct abnormalities, and thus improve the quality of life of the patients. The various materials used in biomedical applications may be grouped into followings:

a) Metals
b) Ceramics
c) Polymers
d) Composites (made from various combination)

1.3 Polymeric Biomaterials

Nowadays, a large number of polymers are widely used in various applications as biomaterials. This is mainly due to the fact that polymers are available in a wide variety of compositions, properties and forms (solids, fibers, fabrics, films, and gels), and can be fabricated readily into complex shapes and structures. However, they tend to be more flexible and weak to meet the mechanical demands of certain applications like implants in orthopedic surgery. They also absorb liquids and swell, leach undesirable products (e.g., monomers, fillers, plasticizers, antioxidants etc.), depending on the application and usage. Moreover, the different sterilization processes like; Ethylene oxide, γ-radiation, electron beam, UV- radiation, etc. may affect more or less the properties of the polymers.

Metals are known for high strength, ductility, and resistance to wear. But many metals show low biocompatibility, corrosion, too high stiffness compared to tissues, high density, and release of metal ions which may cause allergic tissue reactions. Ceramics have good biocompatibility, corrosion resistance, and high compression resistance. Drawbacks of ceramics include brittleness, low strength, difficult to fabricate, low

mechanical reliability, and high density. Polymer composite materials are alternative choice to overcome many shortcomings of homogeneous materials mentioned above. Considering the structural or mechanical compatibility with tissues, metals or ceramics are used for hard tissue applications and polymers for the soft tissue applications. The elastic moduli of metals and ceramics are higher than that of hard tissues. The major problem in orthopedic surgery is the mismatch of stiffness between the tissues and metallic or ceramic implants. In the load sharing between the bone and implant, the amount of stress carried is directly related with the stiffness. So, bone is insufficiently loaded as compared to the implant. This phenomenon is called stress shielding or stress protection. It is found that the degree of stress protection is proportional degree of stiffness mismatch [7]. By matching the stiffness of implant with the host tissues, we can reduce the stress shielding effect and produce desired tissue remodeling. In this respect polymers became more interesting in orthopedic surgery. Likewise fiber reinforced polymers (polymer composites) are good candidates for orthopedic applications. The other advantages of polymer composite biomaterials are the absence of corrosion and fatigue failure, which is commonly seen in metal alloy implants. Metal alloy and ceramics are radio opaque. In case of polymer composite materials the radio transparency can be adjusted by adding contrast medium to the polymer. Moreover the polymer composite materials are fully compatible with the modern diagnostic methods such as computed tomography (CT) and magnetic resonance imaging (MRI) as they are non-magnetic [8, 9].

1.4 Polyether ether ketone (PEEK)

Polyether ether ketone (PEEK) is a linear and highly aromatic semi-crystalline thermoplastic with an average molecular weight of 80,000-120,000 g/mol. It is hydrolytically stable, resistant to wear, stable in solvents and is abrasion resistant [10]. PEEK offers excellent mechanical performance, even at high temperatures. PEEK resins, coatings, and films can be made to conform to FDA requirements, and are considered safe for repeated use with food contact [11]. PEEK has been proven to maintain mechanical and chemical properties past 3,000 hours in high-pressure steam, and has oustanding stability upon exposure to radiation and withstands most chemicals and gasses [11]. PEEK can also be modified for reinforcemnt via glass or carbon fibers, which further increases its versatility.

PEEK has the repeating unit structure, $(-O-C_6H_6-O-C_6H_6-CO-C_6H_6-)$ as shown in figure 1-1. The scientific name of PEEK is: poly(Oxy-1,4 - phenylene -oxy - 1, 4- phenylenecarbonyl - 1, 4 - phenylene).

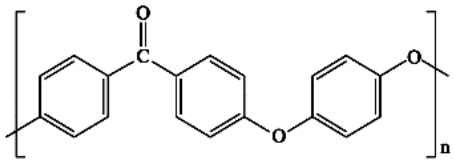

Figure 1-1. Chemical structure of PEEK

PEEK is one member of polyaryletherketone (PAEK) family. The molecular backbone of these polymers contain ketone and ether functional groups between aryl rings. This type of chemical structure of PEEK provides good mechanical properties.

Due to excelent mechanical properties of PEEK, it is used in a wide range of applications such as transportation, energy, industrial, electronics, semiconductors, and medical devices. The introduction of PEEK polymer into the medical field has caused a great deal of interest in the past few years. PEEK is rapidly emerging as a forerunner for high-performance implantable applications. DSC measurements show that the glass transition temperature (T_g) of pure PEEK is about 145℃, and that the melting temperature is about 343℃.

Since the 1980s, polyaryletherketones (PAEKs) have been increasingly employed as biomaterials for trauma, orthopedic, and spinal implants. PEEK has had the greatest clinical impact in the field of spine implant design and is now broadly accepted as a radiolucent alternative to metallic biomaterials in the spine community. The commercial production of PEEK was started when Imperial Chemicals Industries (ICI) filed a patent to make PEEK, called VICTREX® PEEK, in 1978. In 1981, the VICTREX® PEEK ™ polymer family of products including glass and carbon-filled products was commercialized. By the late 1990s, PEEK had emerged as a leading high-performance thermoplastic for replacing metal implants, especially in orthopedics and trauma. In 1998, Victrex launched a carbon fiber-reinforced PEEK. In 2001, Victrex established Invibio® Biomaterial Polymer Solutions to specifically provide medical grades of PEEK [11, 12]. The versatility of PEEK biomaterials increases its complexity for implant designers and researchers seeking to explore new modifications of PEEK for novel implants applications. In recent years, advances in the processing and biomaterials applications of PEEK have been progressing steadily.

PEEK conforms well to the conceptual model of a two-phase, semi-crystalline polymer consisting of amorphous and crystalline phases. Like many semi-crystalline polymers, including ultra-high molecular weight polyethylene (UHMWPE), the crystalline content of PEEK varies depending upon its thermal processing. The crystalline content of injection-molded PEEK ranges from 30% to 35%. In PEEK, bond angle is 125°, and the chain favors a zig-zag conformation (see Figure 1-2) that can form crystallite structures [11, 13].

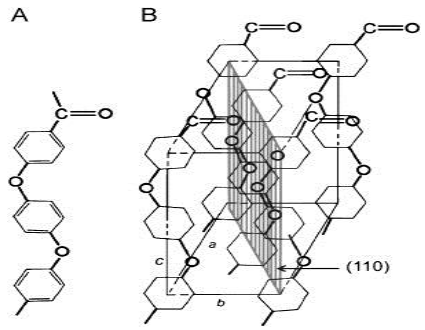

Figure 1-2. (A) Chain conformation of PEEK, and (B) crystal structure of PEEK.

Based on x-ray diffraction studies [11, 12], the unit cell of PEEK shows an orthorhombic structure. The long-axis ("c" in Figure 2), of the orthorhombic unit cell of PEEK spans three aryl groups, with a center-to-center distance of 5Å. PEEK crystals contain very fine lamellae that, under certain conditions, can organize into larger spherulites. The thickness of lamellae, size, and density of spherulites depends on the processing conditions. The mechanical properties of material also depend on the crystallinity which can be affected by temperature, localized cooling rate, and any post-production annealing.

Sterilization is a mandatory process for materials used in medical applications. Sterilization procedures commonly used are steam sterilization, ethylene oxide (EtO) sterilization, and sterilization by radiation. The sterilization of biomaterials may cause chemical and physical change in the materials, such as from crosslinking and chain scission.

Techniques which are used to study effects of sterilization in materials include thermally stimulated luminescence (TSL), electron spin resonance (ESR) spectroscopy, differential scanning calorimetry (DSC), and Fourier transform infrared spectroscopy (FTIR). In this research work, we used TSL and DSC experimental techniques to study the effects of X- and UV-irradiation on PEEK.

The high-energy photons incident upon a polymer can cause chain scission, crosslinking, defects (trapped electrons) within the polymer matrix, and the formation of free radicals. The environmental condition also plays an important role when considering radiation-induced damage. Oxidation can occur in the material if it is exposed to air during or after exposure to radiation. Oxygen can react with free radicals and peroxides can be formed, which may breakdown into more radicals and create other peroxides. This process can increase considerably the amount of free-radicals in the polymer and greatly accelerate the degradation process. Mechanical, as well as structural changes occurring within the polymer may also reduce the longevity of medical implants.

PEEK can be combined with certain additives to create a composite. Carbon and glass are mostly popular reinforcement additives to increase the mechanical properties [14]. PEEK can form a strong interface with carbon fibers, effectively transferring stress between the fibers and the polymer matrix. Due to this excellent property, CFR-PEEK is

currently used in implants for spine fusion and joint replacement. It can also be combined with bioactive fillers like hydroxyapatite (HA) to enhance growth of bone around implants.

1.5 Different Grades of PEEK

PEEK is commercially available in a variety of grades. A variety of implantable PEEK polymers are available, ranging from unfilled grades with varying molecular weight, to image-contrast and carbon fiber-reinforced grades [15]. The different grades of PEEK are listed below.

1) PEEK (Unfilled)

This is a general purpose unreinforced PEEK and has the highest elongation and toughness of all PEEK grades. It has the lowest general mechanical properties (tensile strength, flexural strength, etc.). Unfilled PEEK is compliant with FDA regulation 21 CRF 177.2415 for use in food contact applications.

2) Glass-filled PEEK

Ideal for structural applications, this light-brown variety of PEEK includes the addition of glass fibers which significantly increases its general mechanical properties (tensile strength, flexural strength, etc.), reduces elongation at break, and reduces thermal expansion rates.

3) Carbon-filled PEEK

This variety of PEEK is generally black in color from the addition of carbon fibers, which offers optimum wear resistance and load carrying capabilities. This carbon fiber reinforced (CFR) PEEK further increases PEEK's general

mechanical properties, lowers the thermal expansion rates, and greatly improves thermal conductivity.

4) High Temperature PEEK (HT-PEEK)

This grade of PEEK is light brown in color and is ideal for high-temperature applications. It has a melting temperature of 375°C and a glass transition temperature of 157°C. HT- PEEK shows high temperature performance along with the key characteristics of unfilled PEEK.

Some important properties of different PEEK grades are tabulated below:

Table 1-1. Comparison of some physical properties of different grades of PEEK.

Property	Approximate Value			
	Unfilled PEEK	30% Glass Filled	30% Carbon Filled	HT-PEEK
Density (g/ cm^3)	1.30	1.51	1.40	1.32
Tensile Strength (MPa)	100	150	215	115
Tensile Modulus (GPa)	3.5	11.4	22.3	3.7
Elongation at Break (%)	34	2	1.8	25
Flexural Strength (MPa)	163	212	298	185
Specific Heat (melt) (KJ/kg ℃)	2.16	1.7	1.8	2.2
Glass Transition temperature (℃)	150	150	150	157
Heat Deflection Temperature (℃)	152	315	315	163
Coeff. of Linear Thermal expansion ($x10^{-5}$/℃)	2.6	1.2	1.0	-
Melting Temperature (℃)	343	343	343	374
Thermal Conductivity ($x10^{-4}$ Cal/cm-sec)	6.03	10.3	22.0	-
Transparency/Color	Opaque (Brown)	Opaque (Brown)	Opaque (Black)	Light Brown

All the values of the physical quantities given above are at 23°C temperature [15].

1.6 Background

1.6.1 Unfilled PEEK

Radiation stability is a concern for aliphatic polymers, which are susceptible to bond cleavage during irradiation, leading to the generation of long-lived free radicals [16, 17]. In contrast to aliphatic polymers, because of its aromatic chemical structure, PEEK shows remarkable resistance to gamma and electron beam radiation. Furthermore, even though free radicals are generated during irradiation of PEEK, they rapidly decay: In the study of free radical decay using ESR, Li et al. found no evidence of residual free radicals in PEEK immediately after γ-radiation exposure up to 600kGy, indicating that any free radicals produced by irradiation of PEEK had a lifetime of less than 20 minutes [18]. Much research has been done on PEEK and its composite forms (such as carbon fiber/PEEK composites). The effect of gamma and electron beam irradiation under vacuum on the gas evolution of several aromatic polymers, including PEEK, was conducted by Hegazy et al., who found that crystalline PEEK yielded less gas than amorphous PEEK, and crystalline PEEK then, had better resistance to ionizing radiation [19]. The major evolution gases CO_2 and CO showed that the ether and ketone groups in PEEK chains are affected by radiation, and H_2 evolution indicated the occurrence of crosslinking. They concluded that the aryl ether ketone linkages were seen as exhibiting protective effect against radiation [19].

In other research, Sasuga and Hagiwara hypothesized a higher electron beam radiation resistance for amorphous PEEK than semi-crystalline PEEK, based on dynamic relaxation results [20]. They observed variations in the materials' relaxation behavior at the γ-transition (-100℃), β′-transition (40℃), β-transition (140℃) and α′-transition

(180℃). The authors suggested that the disintegration of tie molecules at the amorphous and crystalline interface would explain the lesser radiation resistance of semi-crystalline PEEK. They also used dynamic viscoelastic properties as indicators of damage due to electron beam radiation. They found that the radiation caused chain scission and allowed the newly created chain ends to loosen the molecular packing to that of a more amorphous polymer. Similar results were obtained by Yoda and Kuriyama for linear polyethylene by x-ray diffraction data [21]. They found that the crystal sizes in polyethylene decreased almost linearly with increasing radiation dose, suggesting that degradation by high energy electron beam radiation may induce chain scission and crosslinking simultaneously. This combined effect resulted in a looser crystal structure and decreased ability to crystallize.

In 1995, Vaughan et al. observed that 66 MGy electron beam irradiation slightly affects PEEK crystallinity [22, 23]. At much higher doses such as 260 MGy, they found that only a small fraction of the crystals were able to recrystallize, and proposed that the formation of intermolecular crosslinks above 260 MGy can occur to such an extent that no melting endotherm can be detected on DSC. However, diffraction patterns and transmission electron microscopy (TEM) still indicated some local orderings in the form of lamellae that could be associated with the crystalline structure of PEEK. The authors concluded that there was likely enough crosslinking within the amorphous regions that the melting of the remaining crystals was prevented.

The effect of heat and electron-beam (e-beam) irradiation on PEEK was studied by K. Shinyama and S. Fujita with the help of dielectric and thermal measurements [10]. They observed an increase in glass transition temperature (T_g) due to e-beam irradiation

above the dose of 100MGy and heat treatment, and concluded that e-beam and heat treatment resulted in crosslinking among the molecules via free radicals in the material. Likewise, Richaud et al. [24] found that the thin samples (60μm) of PEEK undergo mainly chain scission process whereas thick ones (250μm) underwent mainly crosslinking.

P. D. Share et al. reported thermoluminescence around the glass transition temperature (147°C) for gamma-irradiated PEEK fibers [25]. They also reported that there was no change in intensity and shape of the glow curves whether the samples had been irradiated in nitrogen or in air.

Chemiluminescence studies on the thermo oxidation of PEEK at 110℃ were conducted by Brauman and Pronko, who observed no change in properties or accumulation of oxidation products [26]. Evidence suggested that upon exposure to oxygen there was a radical aromatic substitution reaction on PEEK via radical transfer - primarily involving phenoxy radicals. The authors suggested that similar substitution-type bio-molecular termination of phenoxy radicals could account for the oxyluminescence spectrum of PEEK.

Zhang et al. did a systematic study on the tribological behavior of PEEK [27] including estimation of friction coefficients and wear rates. Their results showed that PEEK coatings exhibited an excellent tribological performance with a relatively low coefficient of friction and low wear rate, and that the semi-crystalline PEEK coating exhibits a lower friction coefficient and wear rate than the amorphous one.

If the temperature varies substantially as a function of location in an implant component as it is cooled from the melt, the crystallinity may be spatially heterogeneous, with the

surface "skin" exhibiting potentially lower crystallinity than the bulk core. The introduction of composite fillers like carbon fiber to PEEK can provide additional nucleation sites within the polymer. Crystallization occurs in amorphous PEEK at temperatures approaching (T_g ~143℃), but still far below the principal crystalline melt transition at 343℃. For industrial applications where PEEK may be extensively exposed to high temperatures, "in-service crystallization" may occur [28, 29]. For implant applications, however, temperatures remain well below the glass transition temperature, so in-service crystallization is not a concern.

PEEK exhibits outstanding chemical resistance; the aryl rings are interconnected via ketone and ether groups located at opposite ends of the ring (para position). The resonance-stabilized chemical structure of PEEK results in delocalization of higher orbital electrons along the entire macromolecule, making it extremely unreactive and inherently resistant to chemical, thermal, and post-irradiation degradation.

The thermal stability of PEEK has been studied because of its high-temperature industrial applications and processing conditions. Hay and Kemmish, in 1987, found that thermal degradation occurs in PEEK at temperatures between the glass transitions (T_g) and melt transition (T_m) temperatures, but higher temperatures are needed to produce volatile degradation products [30].

1.6.2 Carbon fiber reinforced PEEK (CFR-PEEK)

Research has been done on CFR-PEEK because of its excellent mechanical properties over wide range of temperatures. Ana M. Diez-Pascual et al. (2009) studied the morphology, thermal, and mechanical properties of PEEK/Carbon nanotube composites [31]. Thermo gravimetric observations indicated an improvement in the

thermal stability of the matrix. DSC measurements showed a decrease in the crystallization temperature with increasing carbon nanotube content (CNT). Likewise, the dynamic mechanical analysis showed an increase in the rigidity of the system with increasing CNT content. The addition of carbon nanotubes shifts the glass transition temperature to higher values, so higher thermal stability and mechanical strength were found for composites with improved dispersion of CNT contents.

Sandra Utzschneider et al. studied the biological response of two different kinds of carbon fiber-reinforced (CFR) PEEK (30% pitch fibers CRF-PEEK LT1 CP 30, and 30% polyacrylonitrile (PAN) CRF-PEEK LT1 CA 30) and compared them with ultra-high molecular weight polyethylene (UHMWPE) in vivo as a standard bearing material [32]. They observed a higher biological response to the two CRF-PEEK materials than for UHMWPE and concluded that CRF-PEEK was an attractive bearing material for arthroplasty.

The wear performance of PEEK-carbon fabric composite was studied by M. Sharma et al. [33]. They developed composites with untreated and cold remote nitrogen-oxygen (0.5%) plasma (CRNOP) treated carbon fabric (67-68 wt %) and PEEK. It was observed that surface-treated fabric composites had much better mechanical (tensile, flexural, and inter laminar shear strength) and tribological properties than untreated fabric. For these composites, a low coefficient of friction (0.21-0.28) and wear rate (~$1x10^{-15}$ m^3/Nm) was observed. The enhanced fiber-matrix adhesion was found to play an important role in improving the performance properties.

Stability and limitations of carbon-fiber reinforced PEEK composites as bearing surfaces for total hip joint replacement have been investigated by A. Wang et al. [34].

The wear behavior of the composite was studied under high-stress, non-conforming contact conditions to simulate total knee contact, and low-stress conforming contact conditions to simulate total hip contact conditions. It was found that CFR-PEEK composites offer a superior resistance over UHMWPE against either metal or ceramic heads in a ball-in-socket contact situation, such as in the hip joint. Pitch-based carbon fibers were found to be superior to PAN-based carbon fibers, while ceramic heads were superior to metal heads. In a high-stress, non-conforming contact situation, CRF-PEEK composites perform poorly as compared to UHMWPE. So, the authors recommended that carbon-fiber composite materials should not be used as a tibial component for a total knee joint replacement.

Chemical resistance of carbon fiber reinforced PEEK and polyphenylene sulfide composites were studied by Ma et al. in 1992 [35]. They studied the aircraft fluid and chemical solvent resistance of CRF-PPS and CRF-PEEK composites. In this work, hydraulic fluid, paint stripper, JP-4 jet fuel, methyl ethyl ketone (MEK), and methylene chloride were taken, and the weight gain of the composites as a function of time were measured. They found that paint stripper degraded the mechanical properties of the composites more than the other solvents and aircraft fluids. It was also observed that the crystallization was enhanced in the presence of these solvents.

A. Almajid et al. investigated the surface damage characteristics and specific wear rates of a continuous carbon fiber reinforced PEEK composite under sliding and rolling contact conditions [36]. In this work, the three different fiber orientation directions (parallel, normal, and antiparallel) were studied by the use of scanning electron microscopy (SEM). Wear tests were also conducted against smooth steel surfaces for

both contact conditions: normal fiber orientation had the lowest specific wear rates in the case of rolling contact; parallel orientation had the lowest specific wear rate in the case of sliding contact.

Godara et al. used nanoindentation and nanoscratch tests to evaluate the effects of sterilization on the micromechanical properties of carbon fiber-reinforced PEEK composites for bone implant applications [37]. In this study, steam and gamma-sterilization were applied, and the results showed that neither steam nor gamma sterilization changed the elastic modulus, hardness or coefficient of friction significantly. However, minor material changes within the PEEK matrix was observed in the interphase regions. It was also found that steam sterilization had a greater influence in the interphase region and slightly increased the thickness of the interphase zone.

1.7 Motivation for Present Study

Existing literature primarily contains information on the effect of γ- and e-beam irradiation on PEEK. Mostly, they have used ESR, FTIR, DSC, XRD, and TEM as experimental techniques to characterize PEEK [18, 22, 23, 44, 43]. However, in this thesis we have used TSL analysis to study the effect of X- and UV-irradiation and preheating on different grades of PEEK. TSL is old but a sensitive experimental technique to study defects and effect of radiation. TSL techniques can also be used to study the phase behavior and transition in polymers, and no detailed TSL study has been previously performed (to our knowledge) in PEEK. In most of the applications this material (PEEK) got exposed to X- and UV radiation. So, it is important to study the effect of these radiations on PEEK. The purpose of this study is to gain a better understanding of effect of X- and UV-radiation on different grades of PEEK by TSL

experimental technique. Finally, we will obtain DSC heating curves to find glass transition, crystallization and melting temperature of different PEEKs before and after irradiation and try to correlate the findings of TSL and DSC measurements.

CHAPTER 2

Theory

2.1 Thermoluminescence or Thermally Stimulated Luminescence (TSL)

Luminescence phenomena in solids, like florescence, phosphorescence and TSL have been studied for many years. Luminescence is the emission of light from an object following initial absorption of energy from some form of radiation. The emission is deemed florescence if the characteristic lifetime τ between absorption and emission is such that, $\tau \leq 10^{-8}$ S, and phosphorescence is characterized with $\tau \geq$ a few seconds [38]. Thermoluminescence in solids is the light emission (mainly visible) that takes place during the heating of a solid following an earlier absorption of energy from radiation. It is in fact the release, in the form of light, of previously absorbed energy and is quite different from incandescence light emission from a substance that is heated at high temperatures. Once thermoluminescence emission has been observed, the material will not show it again after simply cooling the material and reheating it, but has to be exposed to radiation to obtain TL again [39]. It is based on the excitation of electron in a material which becomes trapped then thermally stimulating the electrons to de-excite to the lowest energy state or equilibrium. Once charge carries are initially created they may remain stable for many years before thermal de- excitation. TSL involves two steps. First, a sample must be exposed to ionizing radiation, then the sample must be heated, which yields light emission, collected by a photomultiplier tube (PMT) and current amplifier. Total light output as a function of temperature is called the glow curve, which usually exhibits several maxima. A typical glow curve containing single maximum temperature (T_m) is shown in Figure 2-1.

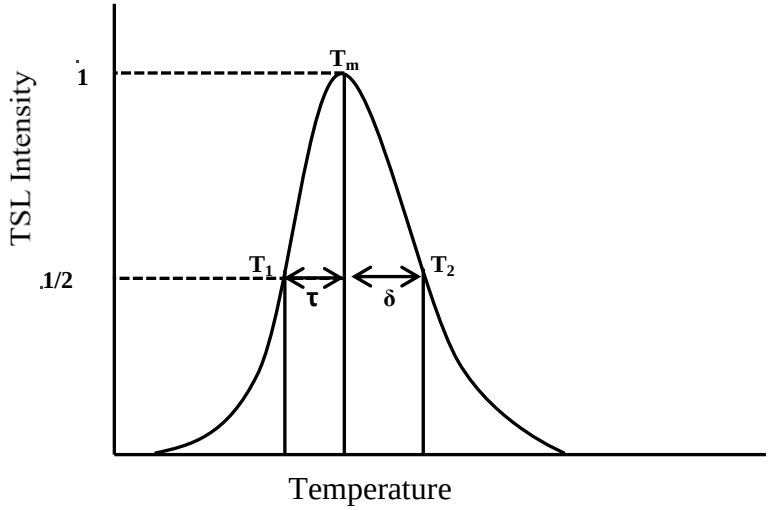

Figure 2-1. A typical TSL glow curve.

The shape of glow curve also depends on the rate of heating. In the figure, the symbols τ and δ represent low and high temperature half width half maximum (HWHM). The temperature T_1, T_2, and T_m are the lower and upper temperatures corresponding to half peak intensity and peak temperature respectively.

Also, $\tau = T_m - T_1$ and $\delta = T_2 - T_m$

The activation energy can be determined by knowing the values of T_1, T_2, and T_m.

2.2 Thermoluminescence Models

Depending on time interval, there are two classes of luminescence- fluorescence and phosphorescence. Phosphorescence and Thermoluminescence are due to one and the same process, the only difference being the fixed and rising temperature respectively of the emitting material during emission.

The presence of traces of an impurity thermally inducted into the host lattice and the structural defects create discrete energy states within the forbidden energy gap of the material. Due to this, radiative recombination may take place and gives rise to

luminescence. These defects are known as luminescent centers. The different models to explain luminescence are explained below:

2.2.1 Jablonski Model

This model was proposed by Jablonski (1935) [38]. According to this model, the luminescent centers of the solid are raised to excited state by absorbed radiation, and then return to the ground state with the emission of light (fluorescence). The system in the excited state can also make a transition to a metastable level (trap), where it can remain until it is returned to ground state. This gives rise to phosphorescence (delayed emission). Fluorescence is temperature independent whereas phosphorescence is dependent of temperature. The phosphorescence emission is delayed by time τ, which is given by the relation:

$$\frac{1}{\tau} = s \exp\left(\frac{-E_t}{K_B T}\right) \tag{2.1}$$

Where, s is a constant, K_B is Boltzmann's constant, T is absolute temperature, and E_t is trap activation energy.

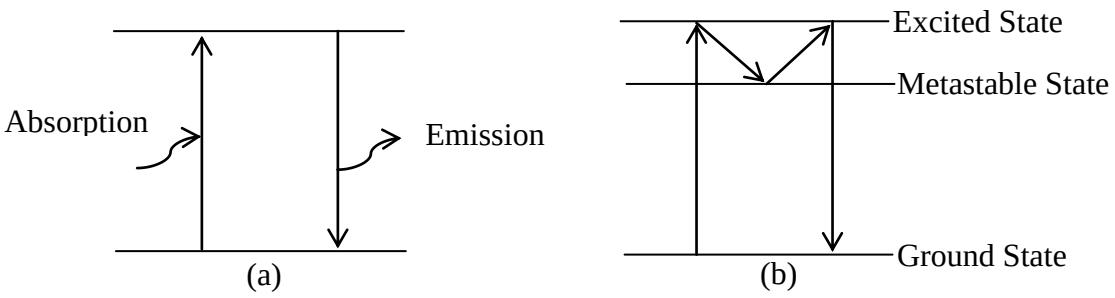

Figure 2-2. Jablonski's model for: (a) Fluorescence, and (b) Phosphorescence.

2.2.2 Configurational-Coordinate Model

This model was first proposed by von Hippel (1936) and applied by Seitz (1939). In this model the vibrational states in the ground state (U_g) and excited states (U_e) of the emission center represents the configuration diagram (Figure 2-3).

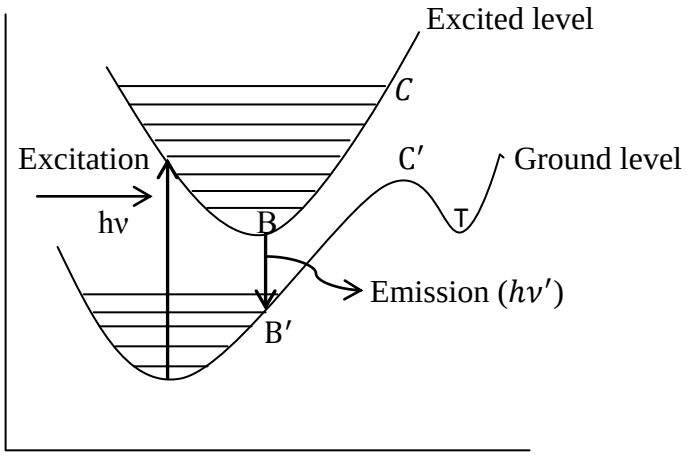

Figure 2-3. Configurational Coordinate Diagram

With the absorption of energy (irradiation), the center will be raised to the excited state (higher vibrational state) and then relaxes to the stable ground state with the emission of radiation. The excited center may also trapped at T through CC', after remaining there for some time τ, it escape to the excited via $C'C$ emitting light via transition BB'. In case of deep traps, energy at room temperature is not sufficient to excite the centers. After heating the irradiated materials will raise trap centers via $C'C$ and the emission output (TSL) through BB'.

2.2.3 Energy Band Model

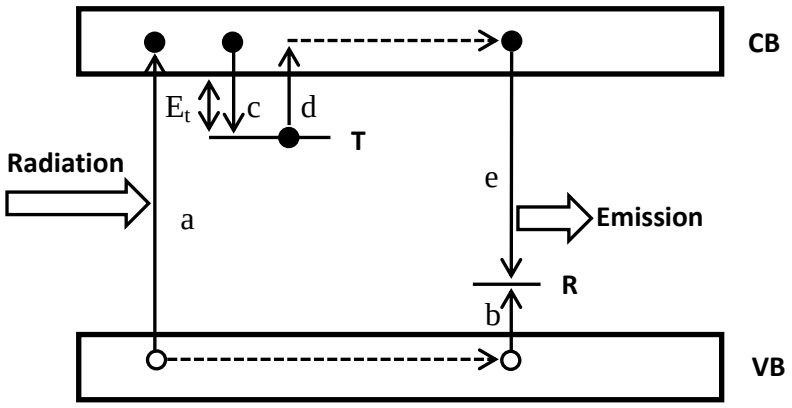

Figure 2-4. A schematic representation of a simple energy-band model in solids.

According to this model, the foreign impurities and defects present in the material is assumed to form the discrete energy levels in the forbidden energy gap. These discrete energy levels acts as traps that can capture charge carriers (electrons/holes) before their recombination with luminescent centers, thereby delaying the luminescence. In the figure, T is trapping level and R is recombination center. If the traps are deep enough (large E_t), the charge carriers will stay for longer time even after irradiation at room temperature. When the temperature of material is increased, charge carriers escape from the traps and recombine with luminescent center (R-state) giving TSL output. As the temperature is gradually increased, intensity of TSL also increases, becomes maximum and then starts to decrease until it becomes zero when all the traps are empty. Here, E_t is called activation energy or trap depth [38, 39].

The probability per unit time of release of an electron from the trap is assumed to be described by the Arrhenius equation,

$$p = s \exp\left\{-\frac{E_t}{K_B T}\right\}$$

Where, s is frequency factor or attempt-to-escape factor, E_t is trap activation energy, K_B is Boltzmann's constant and T is absolute temperature at which electron is stimulated to escape the trap.

2.3 Order of Kinetics

The glow curve kinetics consists of two levels in the elementary theory of TSL for single type of trap and recombination center. They are:

2.3.1 First order kinetics (slow retrapping)

Randall and Wilkins suggested that the rate at which the electron escapes the traps for first order kinetics is directly proportional to the intensity of the glow curve as

$$I_{TL} = ns \exp\left\{-\frac{E_t}{K_B T}\right\} = -\frac{dn}{dt} \qquad (2.2)$$

Where n is the number of electrons trapped at time t. Here, $-\frac{dn}{dt} \propto n$, so it is a first order reaction.

Integrating above equation with respect to time, we get,

$$I_{TL} = n_0 s \exp\left\{-\frac{E_t}{K_B T}\right\} \exp\left\{-\left(\frac{s}{\beta}\right)\int_{T_0}^{T} \exp\left\{-\frac{E_t}{K_B \theta}\right\} d\theta\right\} \qquad (2.3)$$

Where n_0 is initial value of the concentration of the trapped electrons n at t = 0, β is the constant rate of heating, θ is an arbitrary variable representing temperature.

2.3.2 Second order kinetics (fast retrapping)

Garlick and Gibson considered the alternative possibility that re-trapping is fast and developed the expression for the rate of decay as:

$$I_{TL} = \left(\frac{n^2}{N}\right) s \exp\left\{-\frac{E_t}{K_B T}\right\} = -\frac{dn}{dt} \qquad (2.4)$$

Where, N is the number of trapped electrons.

In this case, $\frac{dn}{dt} \propto n^2$. So the equation (2.4) represents second order reaction.

Integrating above equation, we get,

$$I_{TL} = \left(\frac{{n_0}^2}{N}\right) s \exp\left\{-\frac{E_t}{K_B T}\right\}\left[1 + \left(\frac{n_0 s}{\beta N}\right)\int_{T_0}^{T} \exp\left\{-\frac{E_t}{K_B \theta}\right\} d\theta\right]^{-2} \quad (2.5)$$

First and second order kinetics are quantified as 1 and 2 respectively, but there may be intermediate orders as well.

With the fact that the above expressions are not valid for certain situations, May and Partridge developed an empirical expression a general order of kinetics that was later reformulated by Rasheedy as,

$$I_{TL} = \left(\frac{n^b}{N^{b-1}}\right) s \exp\left\{-\frac{E_t}{K_B T}\right\} = -\frac{dn}{dt} \quad (2.6)$$

Where, b is the order of kinetics. Integration gives,

$$I_{TL} = \left(\frac{n_0^b}{N^{b-1}}\right) s \exp\left\{-\frac{E_t}{K_B T}\right\}\left[1 + \frac{s(b-1)\left({n_0}/{N}\right)^{(b-1)}}{\beta}\int_{T_0}^{T} \exp\left\{-\frac{E_t}{K_B \theta}\right\} d\theta\right]^{-\frac{b}{b-1}} \quad (2.7)$$

It is apparent that for b=1 that equation (2.7) will be invalid but it reduces to equation (2.3) for $b \to 1$.

Consider that the above formula for first, second and general order kinetics are quite sufficient to explain TSL phenomena in materials for only a single trapping level as well as a single type of recombination center. A more complex formula is needed to explain multiple trapping sites and recombination centers. Most materials have traps of different depth which implies that for a given temperature deeper traps will exist that have not released the electrons. In the single trap/recombination center formulation the number of trapped electrons was equal to the number of holes (i.e., $n = m$), but in the

case addressed now $n + h = m$, where h is the concentration of electrons in the deeper traps and these deep traps may capture electrons released from shallower traps at E_t. The rate of decay equation now becomes

$$I_{TL} = \frac{ns}{(N+h)}(n + h)\exp\left\{-\frac{E_t}{K_B T}\right\} = -\frac{dn}{dt} \tag{2.8}$$

Expanding, we get,

$$I_{TL} = \frac{s}{(N+h)}nh\exp\left\{-\frac{E_t}{K_B T}\right\} + \frac{s}{(N+h)}n^2\exp\left\{-\frac{E_t}{K_B T}\right\} \tag{2.9}$$

The above equation (2.9) has components of first and second order kinetics. Integrating yields,

$$I_{TL} = \frac{s'h^2\alpha\exp\left\{\frac{hs'}{\beta}\int_{T_0}^{T}\exp\left\{-\frac{E_t}{K_B\theta}\right\}d\theta\right\}\exp\left\{-\frac{E_t}{K_B T}\right\}}{\left[\exp\left\{\frac{hs'}{\beta}\int_{T_0}^{T}\exp\left\{-\frac{E_t}{K_B\theta}\right\}d\theta\right\}-\alpha\right]^2} \tag{2.10}$$

Where, $s' = \frac{s}{(N+h)}$ and $\alpha = n_0/(n_0 + h)$

We can determine the parameters like, activation energy, frequency factor etc. from TSL measurement. The activation energy (E_t) of an electron to escape a trap was determined to be

$$E_t = [2.52 + 10.2(\mu g - 0.42)]\left\{\frac{K_B T_m}{\omega}\right\} - 2K_B T_m \tag{2.11}$$

Where, $\omega = \delta + \tau$ is the full width half maxima (FWHM), δ and τ are the high and low temperature half widths respectively as shown in Figure 2.1, $\mu_g = \delta/\omega$, is a parameter of an asymmetric glow curve which determines the kinetic order. T_m is the maximum peak temperature. The activation energy is the depth of the potential well in which the electron is trapped.

2.4 Thermoluminescence in Polymers

Thermoluminescence in polymer is used to study the molecular motion and structural transitions. We can also evaluate the activation energies or trap depths along with the associated frequency factors. Usually conducted at low temperature (77K), TSL of polymers involves ionizing radiation production of positive ions (luminescent centers) and trapped electrons. When the temperature is increased the electrons become de-trapped through the onset of molecular motion, thermal stimulation, or by tunneling through the potential barriers associated with the traps. The de-trapped electron may be re-trapped if other trapping centers exist along its path to the luminescent center. When the electron finally recombines, it induces an excited state of the neutral luminescent center which then emits a photon as it decays to the ground state.

2.4.1 Electron Traps and Luminescence Centers

In polymers, it is considered to have four types of trapping centers. They are: cavity traps, neutral molecules with positive electron affinity, free radicals, and crystalline region defects [40]. Cavity traps are voids between lamella in the amorphous regions of polymer which release electron due to molecular motion. Neutral molecules with positive electron affinity can act as electron traps if they are in sufficient concentration. The presence of oxygen increases the deep traps due to oxidation products. Free radicals have also been associated to luminescence centers in PMMA. At low temperature, the free radicals will not react and so do not contribute to thermo luminescence.

2.5 Differential Scanning Calorimetry (DSC)

Differential Scanning Calorimetry (DSC) is a technique used to measure thermal properties of polymers based on the rate at which they absorb heat energy compared to a reference material. DSC analyzes thermal transitions occurring in a polymer samples when it is heated or cooled. We can measure glass transition temperature (T_g), melting temperature (T_m), crystallization temperature (T_c), decomposition temperature (T_d) as well as other various transitions can be determined by DSC measurement [41].

The DSC thermogram is the plot between the difference in heat flow and temperature (Figure 2-6). When there is no phase transition in polymer, the plot is parallel to temperature axis. If q is heat supplied in time t then, Heat flow = q/t.

Heating rate is the rise of temperature ΔT per unit time t, so Heating rate = $\Delta T/\tau$

The heat capacity C_p is given by $$C_p = \frac{q/t}{\Delta T/t} = \frac{q}{\Delta T}$$

A typical DSC heating curve is shown in the figure below.

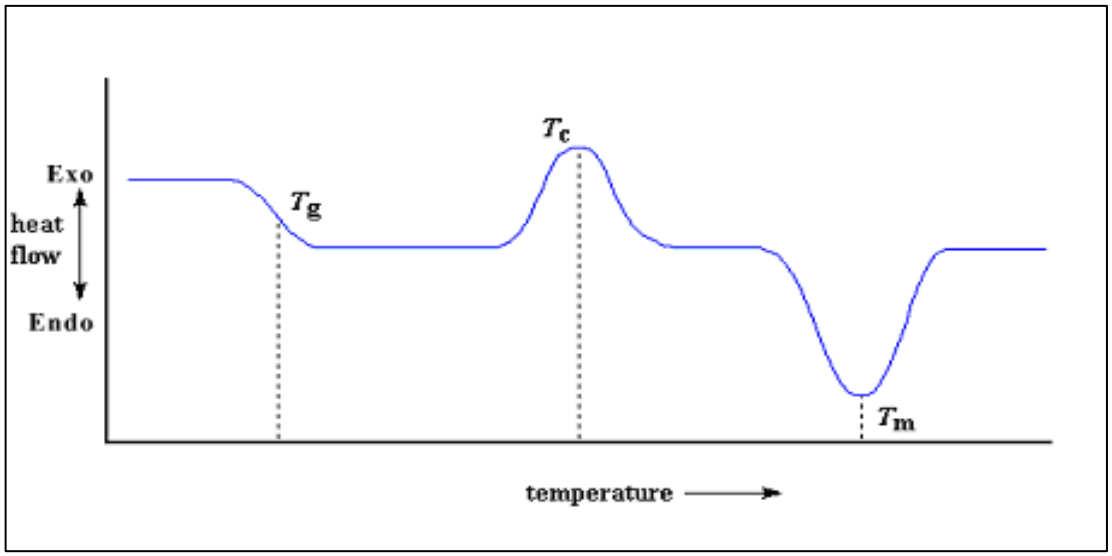

Figure 2-5: A typical DSC heating curve

From the diagram, it can be seen that a sudden upward jump in the curve signifies an exothermic process. A sudden drop in heat flux indicates an endothermic process.

Glass transition temperature (T_g)

This is the point at which, on heating, an amorphous polymer changes from being hard, brittle and glass like to being a soft rubber like substance. At glass transition temperature (T_g), DSC thermogram shows an incline and it is an endothermic process. It is obvious that the heat capacity increases at T_g. No latent heat is associated with glass transition temperature. So the glass transition phenomenon is second order phase transition.

Crystallization temperature (T_c)

Continuing to heat a polymer past its Glass transition temperature eventually leads to another transition. Before this point in the thermal analysis, the molecules are arranged in a random fashion and are coiled around each other in an unfavourable manner. A transition occurs when molecules acquire enough freedom to move into a more energetically stable phase, i.e., a crystalline state. This would indicate that the phase following the glass transition is metastable and when sufficient energy is supplied, its molecules adapt a more stable (lower energy) arrangement. Because the molecules in a crystalline solid have less freedom than in amorphous, the transition between these two states is exothermic. The amorphous solid samples do not show crystallization temperature in DSC graph. This is also a first order transition.

Melting temperature (T_m)

This is the temperature at which the (crystalline) polymer molecules have gained enough vibrational freedom to break free from the solid binding forces and form a liquid.

Due to the increased freedom of these molecules, the DSC graph should take a sudden dip at this temperature to indicate the endothermic nature of the process. This is a first order phase transition.

Degradation Temperature (T_d)

The final transition on a DSC graph is the degradation temperature (T_d). At this point in the heating cycle, individual bonds between atoms start to break as the vibrations become more and more fierce and polymer molecules decompose into their components. Depending on the nature of the substance under investigation, this process can be either endothermic or exothermic.

CHAPTER 3

Materials and Method

In this study we have used four different grades of PEEK samples: PEEK film, PEEK rod, high temperature PEEK (HT- PEEK and Carbon fiber reinforced PEEK (CFR-PEEK).

3.1 TSL measurement

The PEEK-film having thickness of 10 mil (0.254mm) were cut into 2mm x2 mm samples pieces each of masses 2.0 mg to 2.2 mg using a micron 360 mictome (Richard-Allen Scientific) fitted with a tungsten-carbide knife. The remaining three PEEK samples were in the form of rod having 6mm in diameter and were made sample each of mass between 10.0 mg to 10.4 mg. The samples were placed in TSL pans (DSC pan without top) for testing. TSL measurements were carried out using a commercial dosimeter (Harshaw QS 3500) (Figure 3-1) in which heating chamber was continuously purged with dry and filtered Nitrogen gas (N_2) to avoid the production of thermally oxidized radicals and moisture. The samples of PEEK were heated from 40℃ to 350℃ at a rate of 1℃/s. The resulting TSL intensity (glow curve) was recorded as a function of temperature using WinREMS software interface. Each of the glow curves were then deconvoulated into an individual glow peaks using peak-fit software. The glow peak parameters of the individual peaks were then calculated using curve fitting software from Los Almos National Laboratory.

Figure 3-1. TSL experimental setup (Harshaw QS 3500)

A block diagram of TSL reader is shown in Figure 3-2.

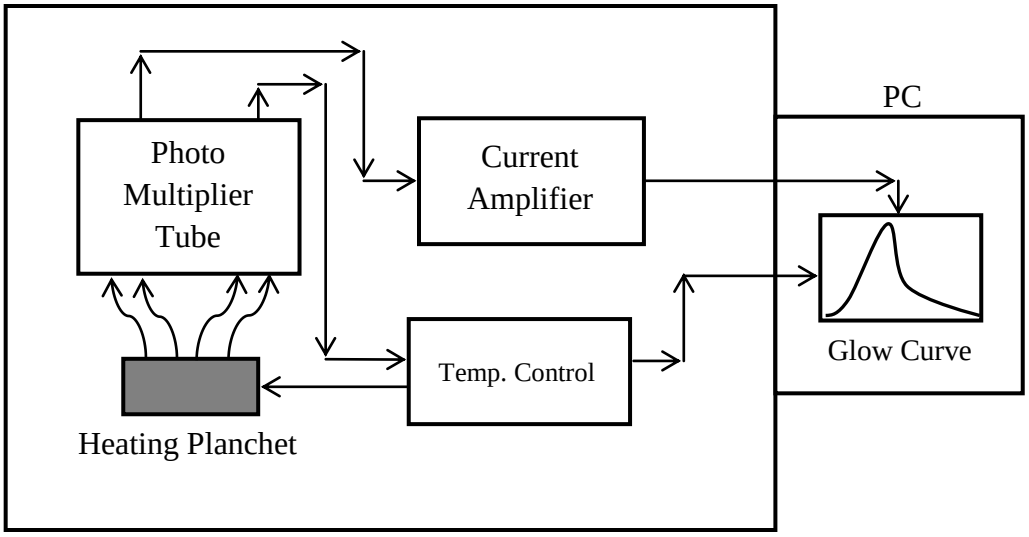

Figure 3-2. A block diagram for TSL reader

3.2 DSC measurement

For all types of PEEK, we have also conducted DSC measurement for irradiated and non-irradiated samples. We are also interested in DSC measurement to investigate

the effect of radiation on PEEK. Previous investigators found that T_g, T_c, and T_m may change with irradiation dose [31, 47, 48].

For DSC measurement, we have used '901 Differential scanning calorimeter' system. In a DSC experiment, two pans are placed on a pair of identically positioned platforms connected to a furnace by a common heat flow path. One pan contain test sample and the other is empty (reference). These pans are heated up at constant rate. The difference in heat flow between sample and reference can be measured and so it is called differential scanning calorimeter (DSC).In this study, DSC measurements were performed at a constant heating rate of 20ºC/min.

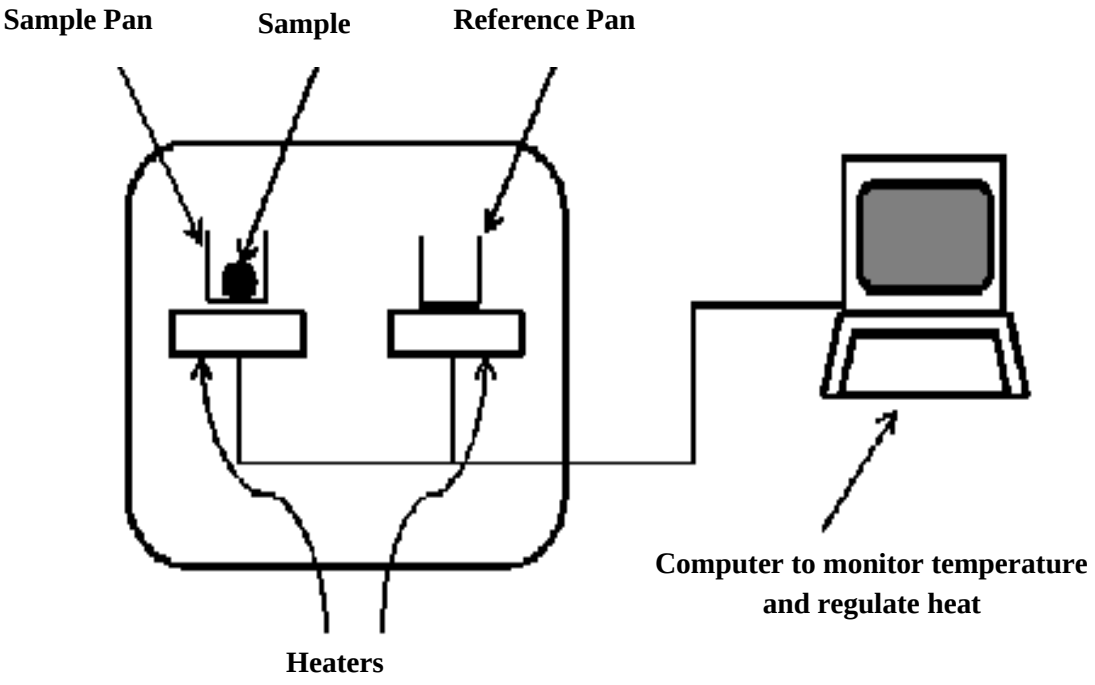

Figure 3-3. Schematic diagram of Differential Scanning Calorimeter

3.3 Groups of PEEK samples

For this study, we have prepared the following groups of samples:

A) PEEK film samples

The samples of mass 2.0 to 2.2 mg were made with the cross-section area of 2mm x 2mm. Then the TSL measurement was done with following irradiation condition.

i) X-irradiated samples

Samples were X-irradiated with 50 KV, 40 mA source at room temperature in air for 10, 20, 30, 40, 50, and 60 minutes.

ii) UV-irradiated samples

Samples were irradiated with wide band UV- source (250 Watt, Oriel® 688 10 Arc Lamp) at room temperature in air. We have used water filter in front of UV source so that UV light passes through the column of water before it reached the sample. The water absorbs thermal heat energy so that the testing samples were irradiated only with UV light. The samples were UV-irradiated for 10 and 20 minutes.

iii) Preheated samples

In order to study the effect of heat on PEEK, we heat the samples of PEEK at different temperatures (150, 200, 250, 300, and 341ºC) for 1 hour in air before the measurement.

iv) DSC samples

For DSC measurement we have used PEEK film sample of masses 5mg. DSC data were obtained for non-irradiated and 1 hour X-irradiated samples.

B) CFR-PEEK samples

i) X- and UV-irradiated samples

Originally, the sample of CFR-PEEK was in the form of rod. So we cut the rod and made the test samples of mass 10mg. These samples were irradiated with X- and UV for 1 hour before testing.

ii) Preheated samples

The samples of mass 10mg were preheated at 200 and 300ºC for 1 hour in air before the measurement.

iii) DSC samples

For this study, samples of mass 10mg were taken and DSC measurement was obtained for non-irradiated and 1 hour X-irradiated samples.

C) HT-PEEK samples

i) X- and UV-irradiated irradiated samples

We cut HT-PEEK rod and make samples of mass 10mg. The samples were X- and UV-irradiated for 1 hour and then tested.

ii) Preheated samples

The samples were preheated at 150, 200, and 300ºC for 1 hour in air before the measurement.

iii) DSC samples

DSC measurement was obtained for non-irradiated and 1 hour X-irradiated samples of HT-PEEK.

D) Unfilled PEEK-rod

i) X- and UV-irradiated samples

We cut unfilled PEEK-rod and make samples of mass 10.0 mg. The samples were X- and UV-irradiated for 1 hour and then tested.

ii) Preheated samples

The samples were preheated at 150, 200, and 300ºC for 1 hour in air before the measurement.

CHAPTER 4

Results and discussion

4.1 TSL analysis of X- or UV-irradiated PEEK.

4.1.1 TSL in PEEK-film

Share et al. reported TSL glow peak around the glass transition temperature (T_g) of 420K (147°C) in γ-irradiated PEEK fibers [25]. They observed one glow peak, which did not change in its intensity or shape whether the γ-irradiation was performed in nitrogen or in air. In our work, UV- and X-irradiation were chosen to study the effects of radiation in PEEK because we can perform these radiation treatments in-house and can observe the effects immediately after radiation exposure.

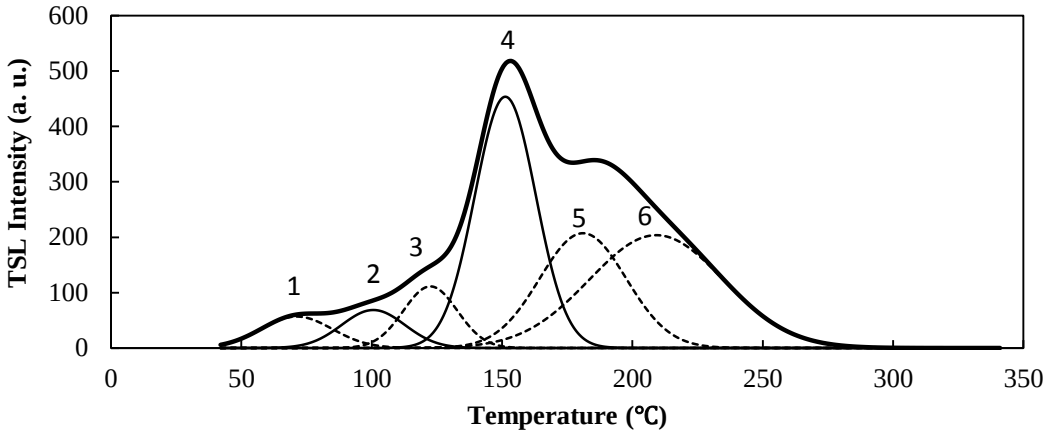

Figure 4-1. TSL glow curve for non-irradiated PEEK film

The glow curve (Figure 4-1) of non-irradiated PEEK film shows a major peak (peak 4) at a temperature of about 150°C (glass transition temperature, T_g), similar the glow curve observed by previous investigators [18, 25]. This deconvoulated TSL glow curve shows six peaks leveled: 1, 2, 3, 4, 5, and 6 at temperatures of about 75℃, 100℃, 124℃, 150℃, 180℃ and 210℃, respectively.TSL glow curves for X-irradiated PEEK

film with peaks of interest (peaks 2 and 4) are shown in Figs. 4-2, 4-3, 4-4, 4-5, 4-6, and 4-7 for different irradiation times.

X-irradiated for 10 minutes

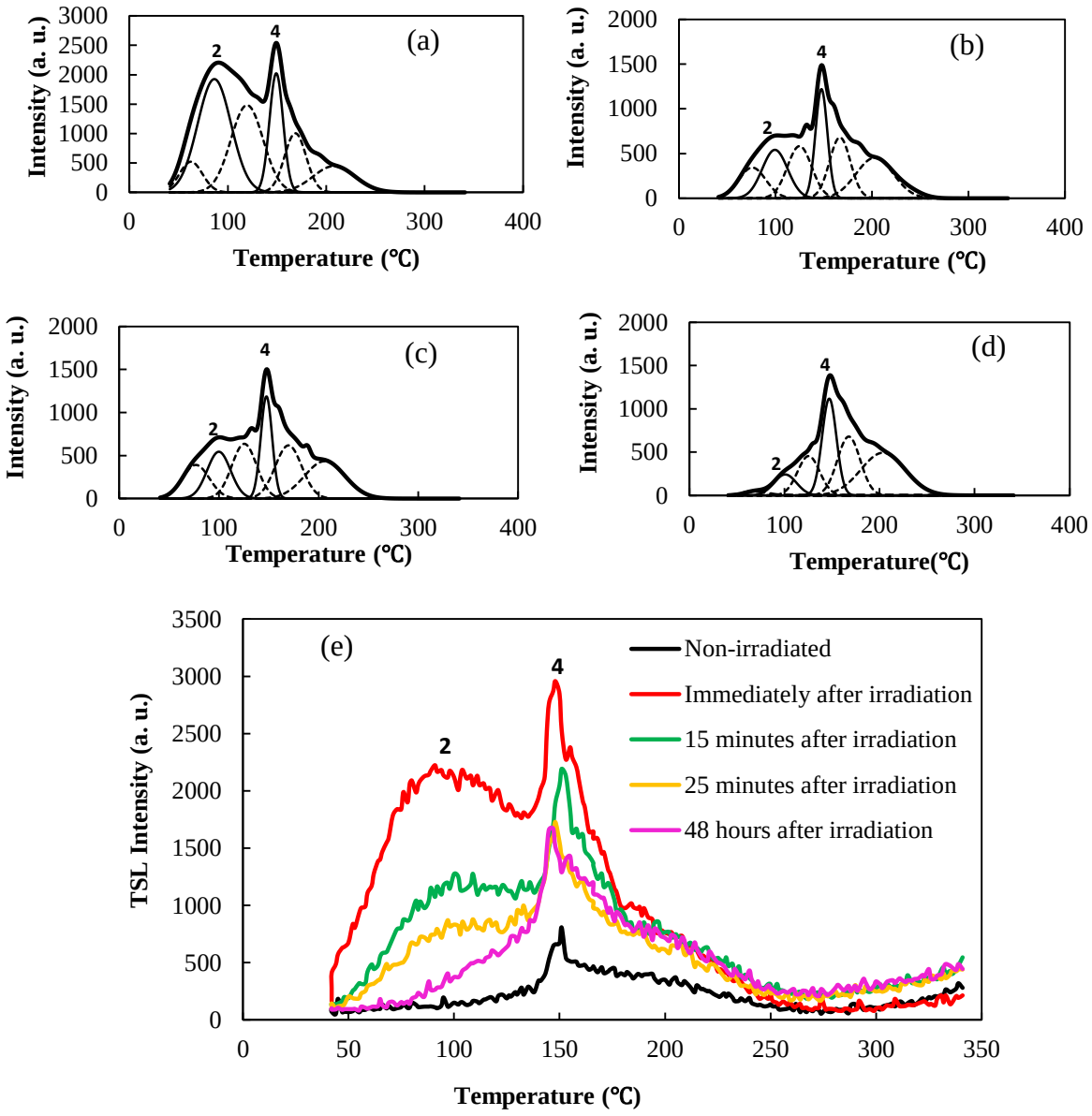

Figure 4-2. TSL glow curves for PEEK film (all are X-irradiated for 10 minutes): (a) Immediately after irradiation; (b) 15 minutes after irradiation; (c) After 25 minutes; (d) 48 hours after irradiation; (e) Combined glow curves.

X-irradiated for 20 minutes

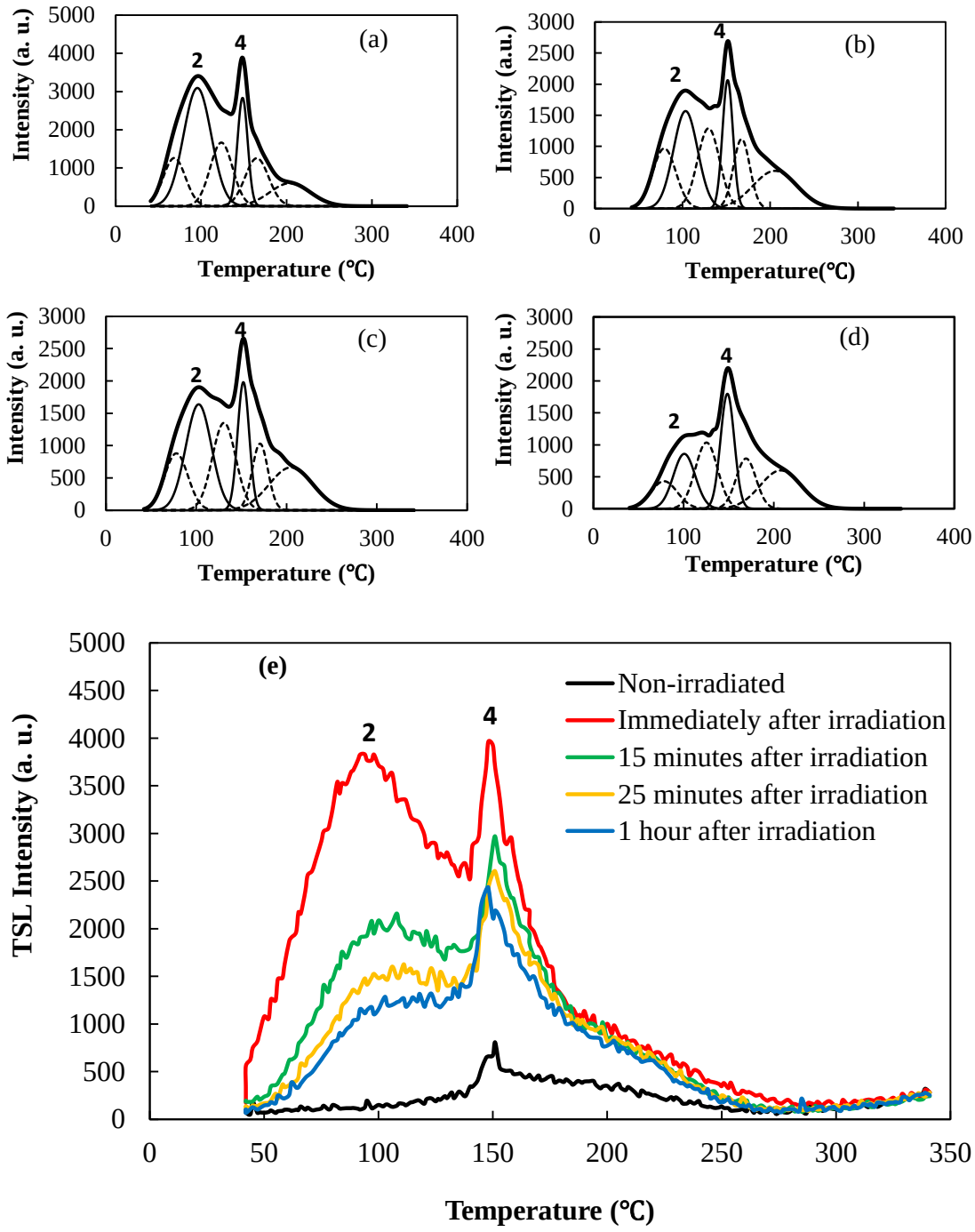

Figure 4-3. TSL glow curves for 20 minutes X-irradiated PEEK film: (a) Immediately after irradiation; (b) 15 minutes after irradiation; (c) 25 minutes after irradiation; (d) 1 hour after irradiation; (e) Combined glow curves.

X-irradiated for 30 minutes

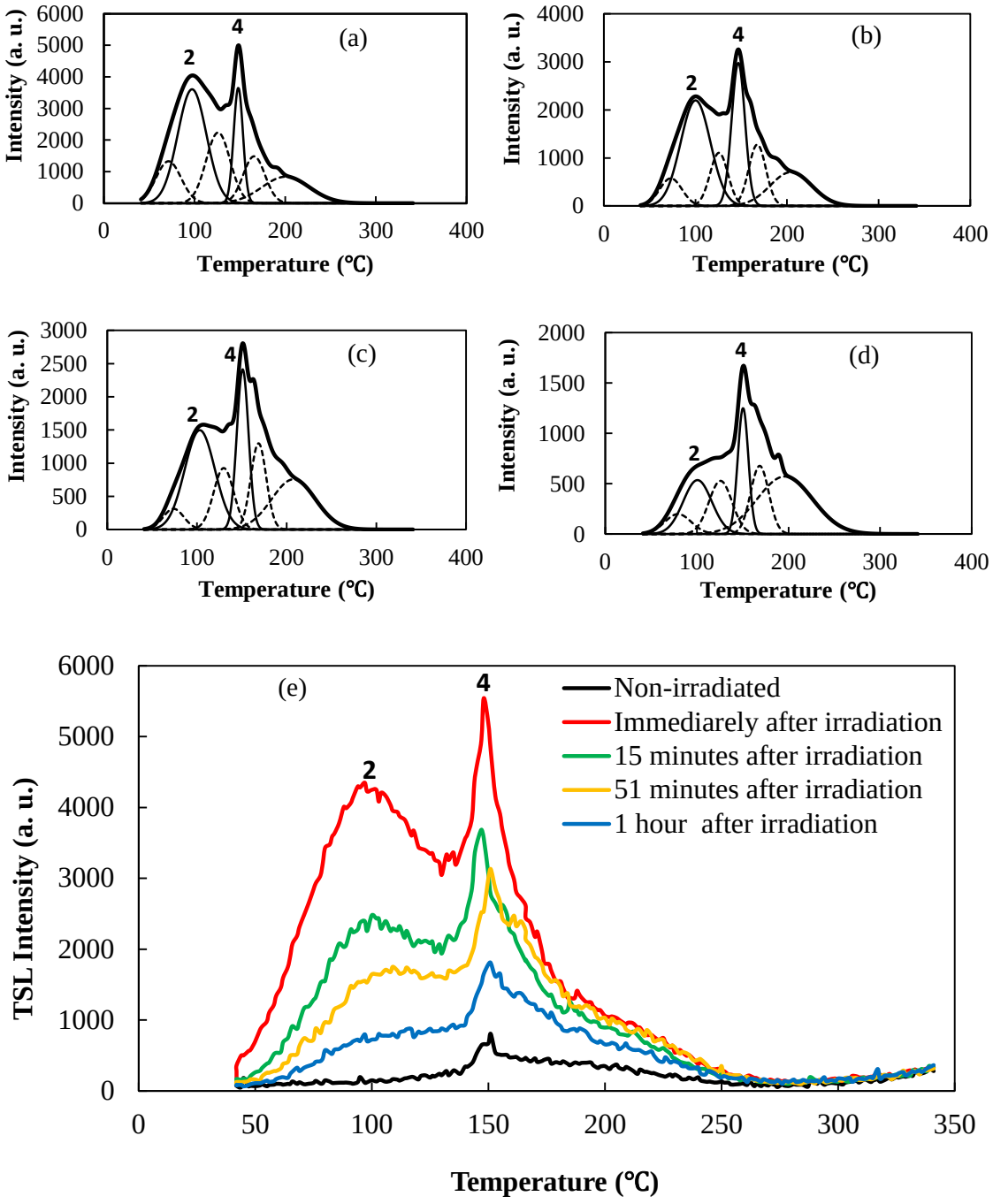

Figure 4-4. TSL glow curves for PEEK film (all are X-irradiated for 30 minutes): (a) Immediately after irradiation; b) 15 minutes after irradiation; (c) 51 minutes after irradiation; (d) 1 hour after irradiation; (e) Combined glow curve

X-irradiated for 40 minutes

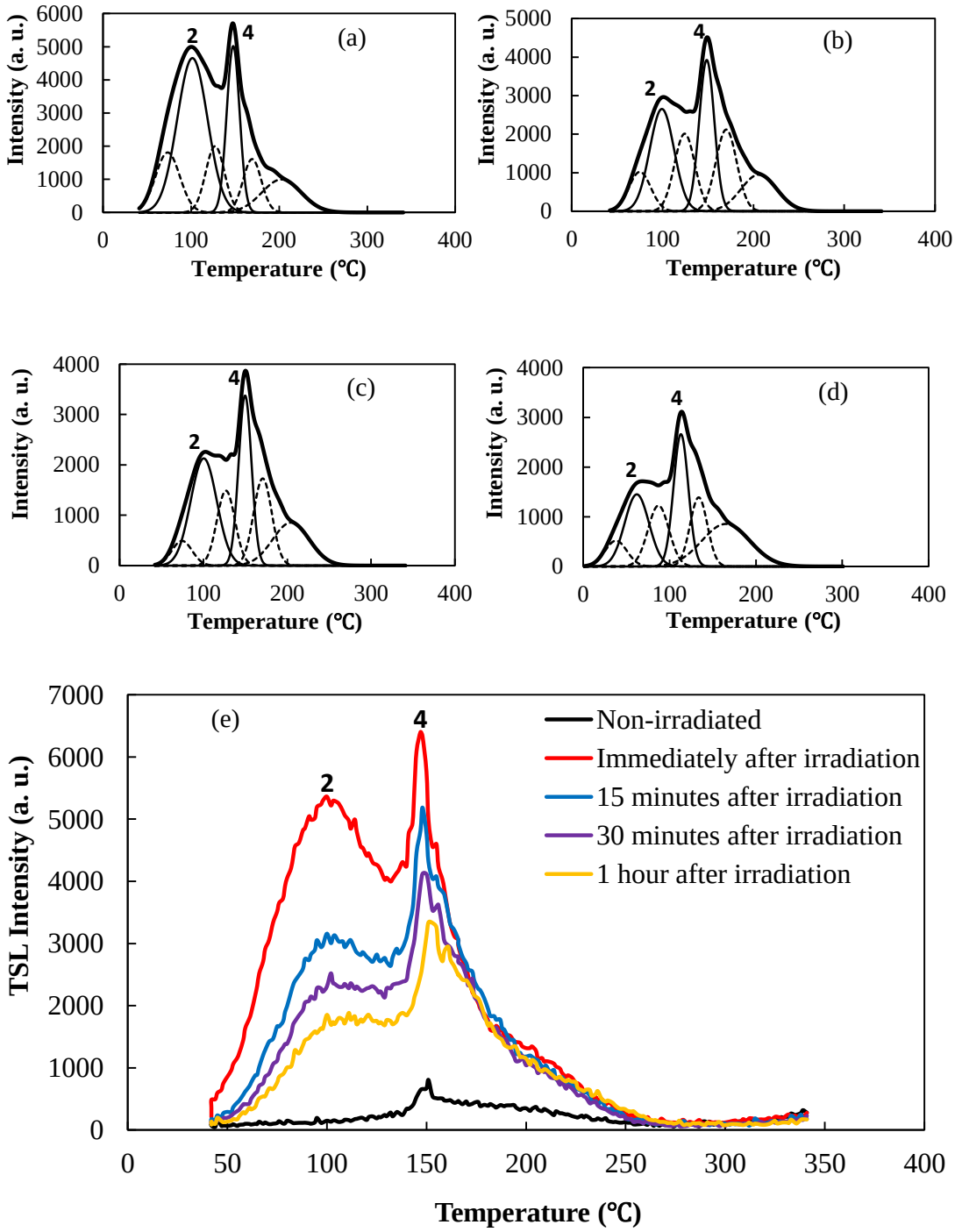

Figure 4-5. TSL glow curves for PEEK film (all are X-irradiated for 40 minutes): (a) Immediately after irradiation; (b) 15 minutes after irradiation; (c) 30 minutes after irradiation; (d) 1 hour after irradiation; (e) Combined glow curves

X-irradiated for 50 minutes

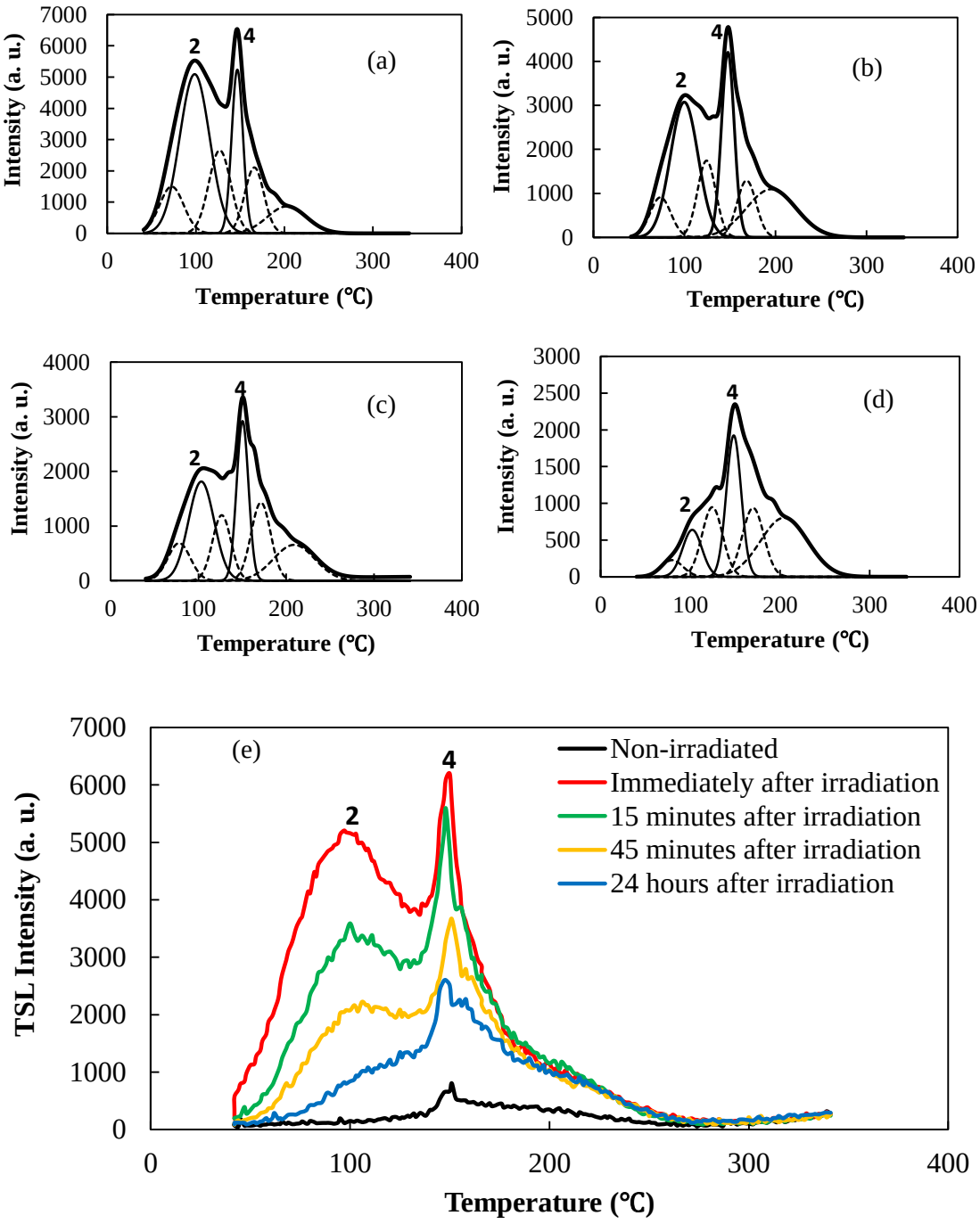

Figure 4-6. TSL glow curves for PEEK film (all are X-irradiated for 50 minutes): (a) Immediately after irradiation; (b) 15 minutes after irradiation; (c) 45 minutes after irradiation; (d) 24 hours after irradiation; (e) Combined glow curves

X-irradiated for 60 minutes

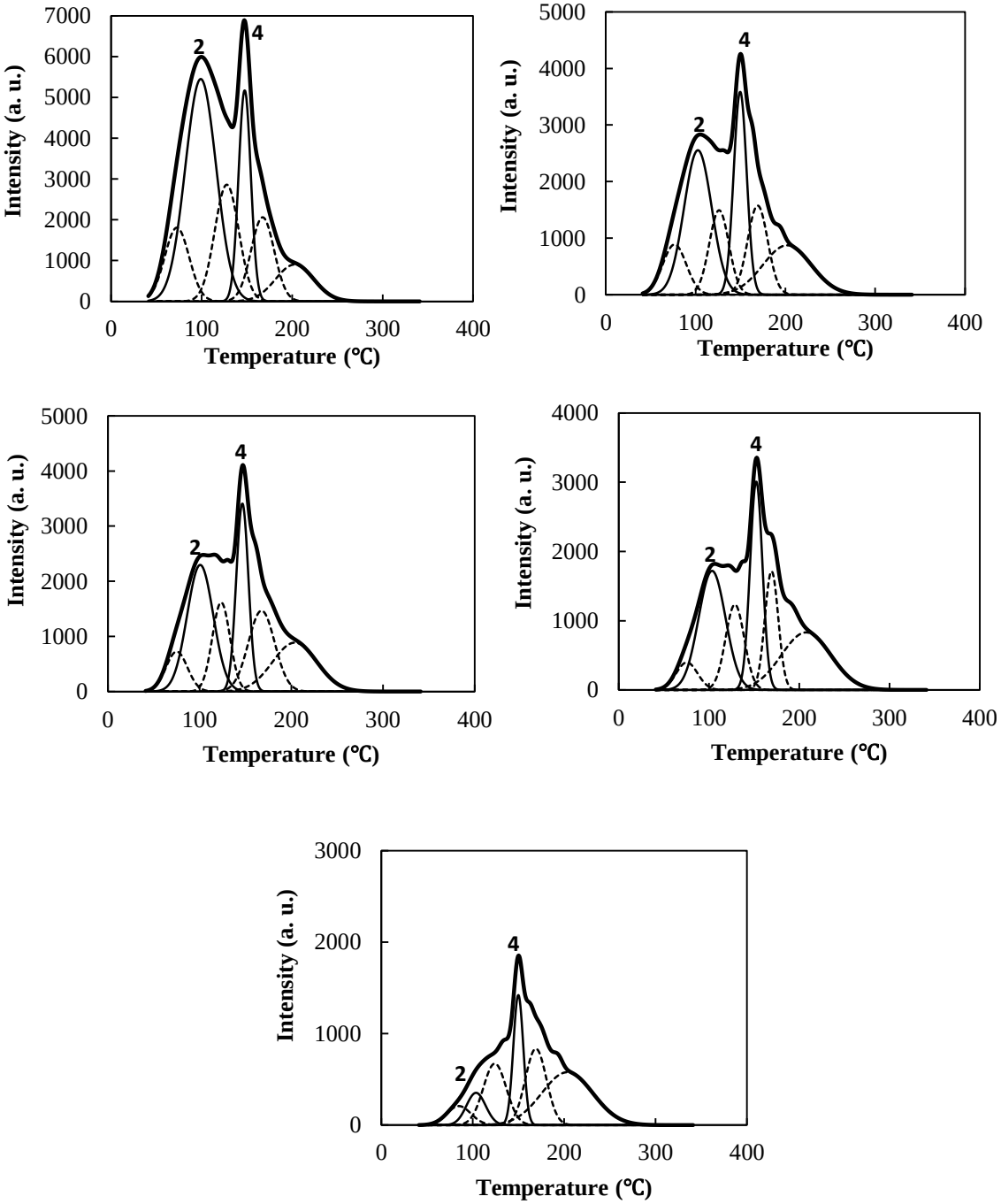

Figure 4-7. TSL glow curves for PEEK film (all are X-irradiated for 60 minutes): a) Immediately after irradiation; (b) 15 minutes after irradiation; c) 33 minutes after irradiation; d) 1 hour after irradiation; (e) 24 hours after irradiation

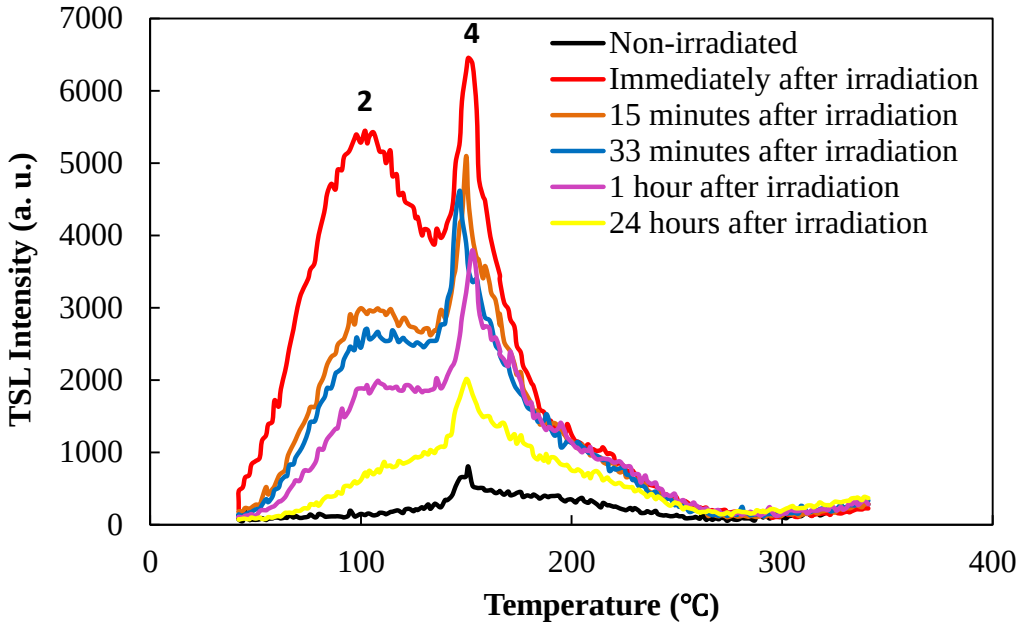

Figure 4-7. (f) Combined glow curves for 60 min. X-irradiated PEEK film.

With the help of Peak fit software to deconvolute the glow curves, a combination of six peaks within each glow curve can be observed. Thermal activation energy associated with these glow peaks ranges between 0.89 eV and 3.2 eV, and the reaction mechanism seem to follow a kinetic order of 1.5. The TSL parameters associated with these peaks are tabulated in appendix. Out of these six peaks, two are major peaks (peaks 2 and 4), which can be observed directly without deconvolution. These peaks (2 and 4) which appear near the temperatures of 100℃ and 150℃, are of primary interest. Peak 4, at 150℃, corresponds to the glass transition temperature of PEEK. Also, from the above glow curves, we observed that the intensities of peaks 2 and 4 increase with X-ray dose (irradiation time). Figures 4-8 and 4-9 (below) show the TSL glow curves for PEEK film samples, and the growth of peaks 2 and 4 with X-ray exposure time. Area under each peak was calculated, and plotted with time of X-ray exposure. From the resulting growth

line, it can be seen that peaks 2 and 4 are mostly saturated (little increase) after 40 minutes.

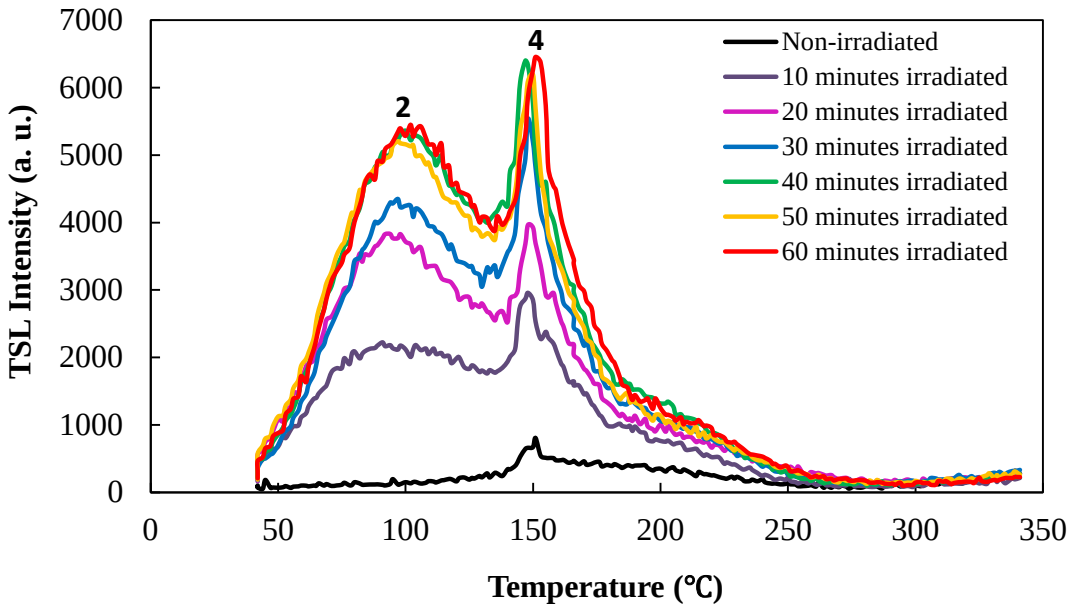

Figure 4-8. Combined TSL glow curves for PEEK (film) for different X-irradiation time

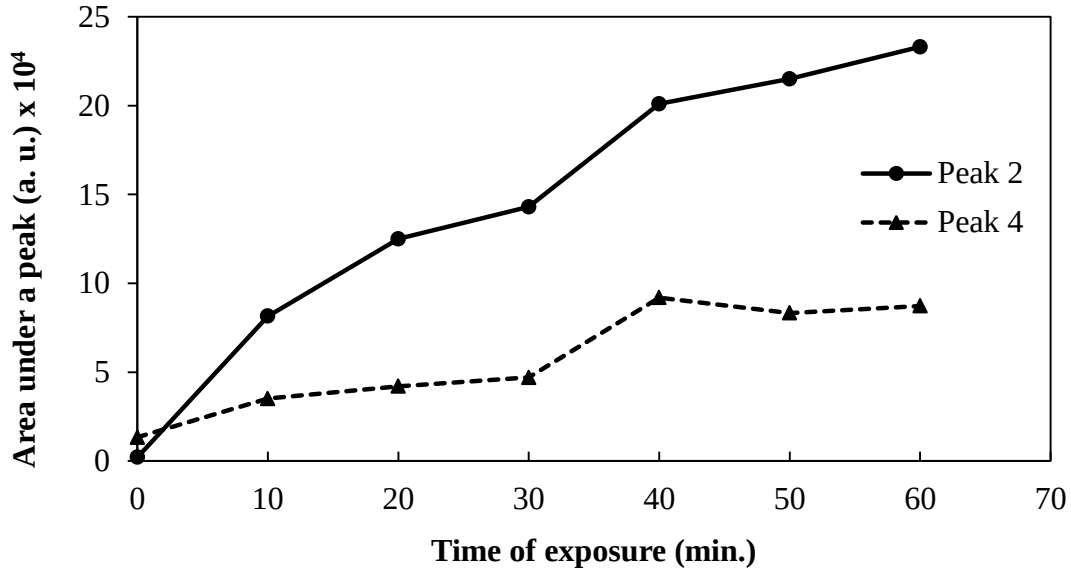

Figure 4-9. Growth of peak 2 and 4 with time of X-ray exposure.

Decay behavior of peaks 2 and 4 are shown in the Figure 4-10.

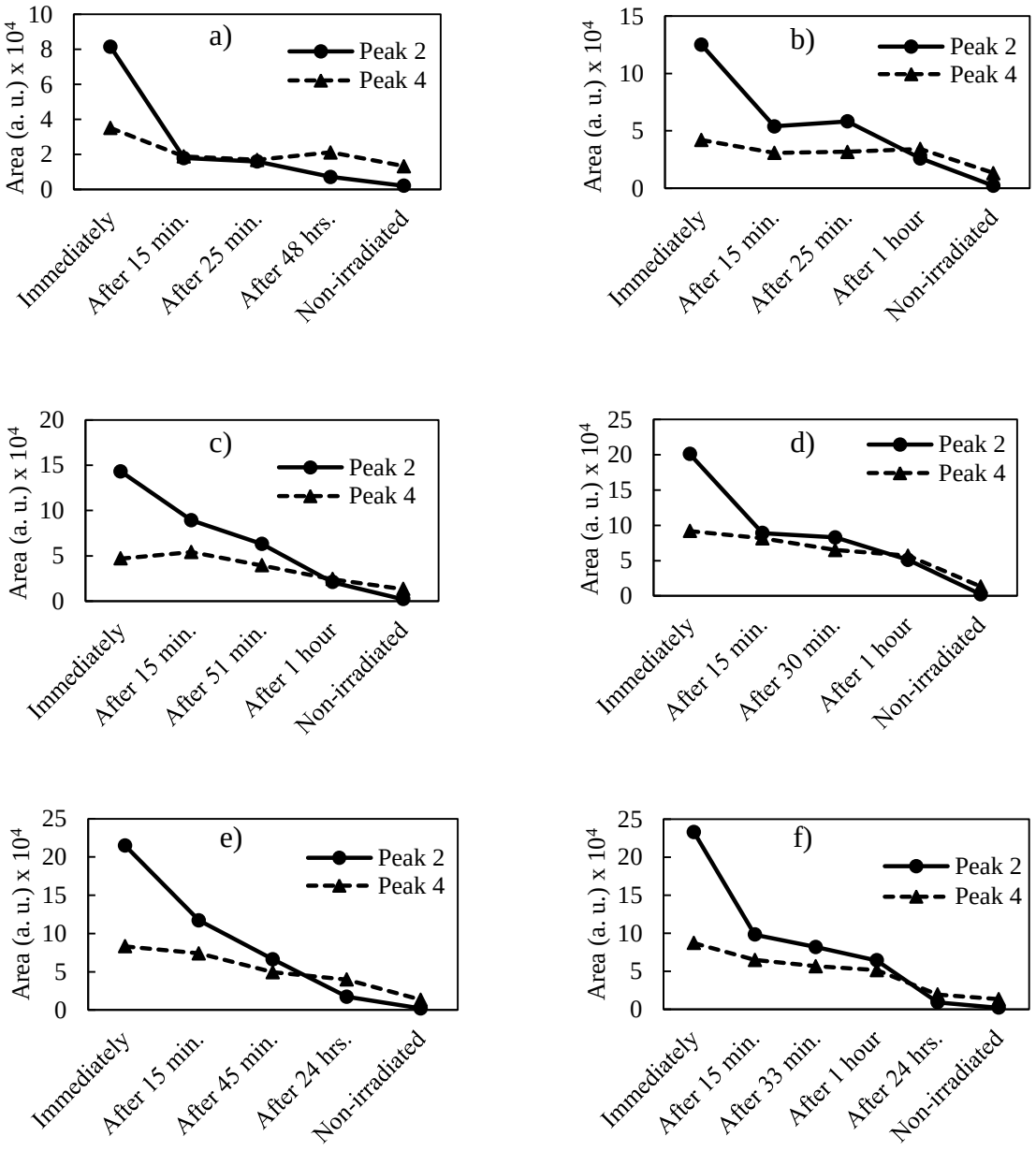

Figure 4-10. Line graphs showing decay behavior for peaks 2 and 4 for X-irradiated PEEK film after different irradiation times. a) 10 minutes, b) 20 minutes, c) 30 minutes, d) 40 minutes, e) 50 minutes, and f) 60 minutes of X-irradiation.

From decay line graph, the area under the peak 4 is initially (before irradiation) greater than area under peak 2. However, peak 2 looks to be much more affected by irradiation such that immediately after radiation the area under this peak much more greater that the area under the peak 4. Also, for all irradiation treatments, the area of peak 2 quickly decreases and becomes smaller than peak 4 within 24 hours - similar to before irradiation. Similar observations were made for UV-irradiated PEEK film samples (Figure 4-11), but there was little increase in the peak intensities with UV exposure time. This may be due to the X-ray's higher energetic radiation, as compared to UV.

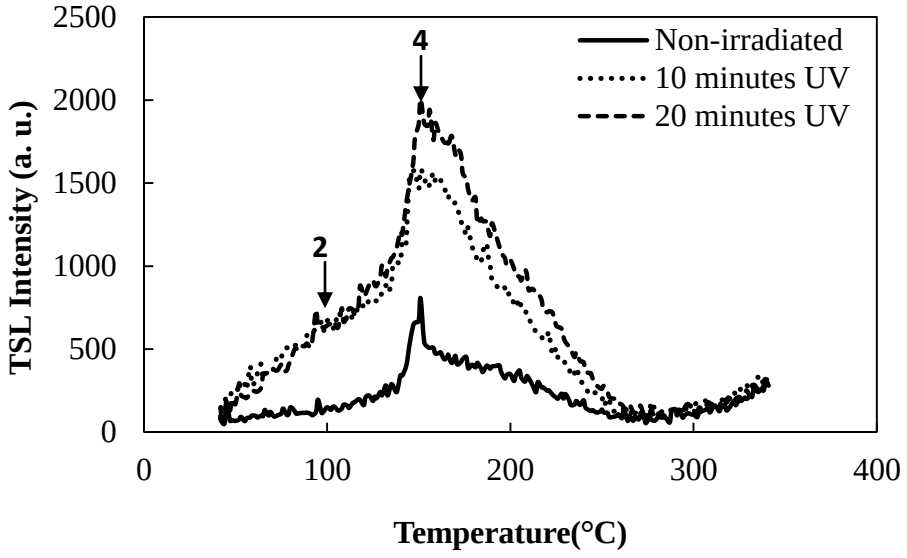

Figure 4-11. TSL glow curve for UV-irradiated PEEK film

It has been previously observed in literature that free radicals can be produced in PEEK when irradiated [31]. These free radicals may act as trapping sites for electrons, and also, the concentration of ionic species may be increased by irradiation. This phenomenon gives rise to larger peaks in the glow curves of PEEK near its glass-transition (T_g) temperature of 150°C, which corresponds with peak 4. It is difficult to

correlate these results for PEEK with other measurements because the change in crystallinity may have had a profound effect on its properties [18]. H. M. Li et al. observed no change in the value of T_g with electron beam irradiation, although the TSDC (Thermally stimulated discharge) increase with the peak moved to higher temperatures. This suggests that this peak is associated with some form of electron capture.

The explanation for the changes in the TSL glow curve (peaks) can be made in terms of relaxation behavior of polymer chain. With the help of dynamic viscoelastic measurement, T. Sasuga et al. [20, 25, 42] showed that PEEK shows excellent radiation resistant (γ-irradiation, e-beam radiation). The aromatic units present in the chemical structure of PEEK make it more radiation resistant. Also, in comparison, non-crystalline PEEK is more radiation resistant than crystalline PEEK. It has been reported that the chains at the interface between crystalline and non-crystalline domains are affected more by radiation than the chains in non-crystalline and/or crystalline phase. The lower radiation resistance of semi crystalline than non-crystalline PEEK is related closely to the disintegration of tie molecules between crystalline and non-crystalline phases. From these observations the authors conclude that the effect of radiation not only depends on the chemical structure of PEEK but also on the order of structure such as the presence or not of crystallites. In this study the authors observed three discrete mechanical loss peaks. γ-relaxation at -80℃, β- relaxation at 150℃ and α′-relaxation at 180℃ for unirradiated non-crystalline PEEK. The low temperature γ- relaxation is assigned to local motion of aromatic units in the main chain in the glassy state. The β- relaxation is attributing to molecular motion reflecting the transition from glassy to elastic state. The α′-relaxation is related to the molecular arrangement from non-crystalline to semi crystalline state (α′

relaxation is not present in PEEK specimen with crystallinity greater than 15%). Also it was observed that for e-beam irradiation, the temperature corresponding to β and α′ relaxations shift to the higher temperature with the increasing dose. These observations suggest that irradiation cause cross-linking in the polymer chain. For irradiated PEEK a new peak was observed (β′ relaxation) just below the glass transition temperature. This β′ relaxation was assigned due to movement of the main chains during rearrangement from loosened chain packing to a more rigid chain packing [20, 42, 43].

4.1.2 TSL in CFR-PEEK

TSL glow curves for carbon fiber reinforced PEEK (CFR-PEEK) in UV- and X-irradiation is shown in Figure 4-12.

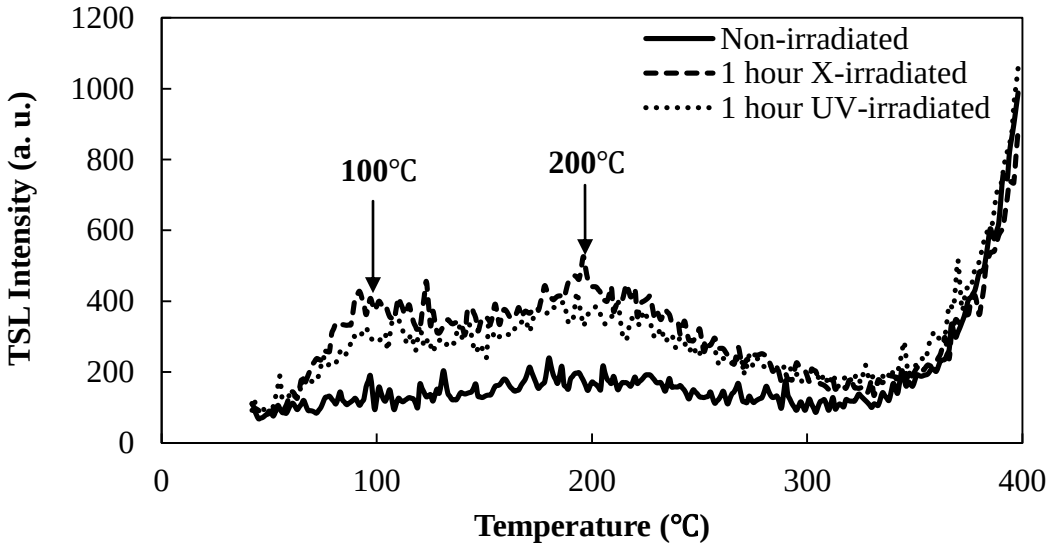

Figure 4-12. Glow curves for UV- and X-irradiated CFR-PEEK.

Non-irradiated CFR-PEEK showed no luminescence output, which indicated that there were no active species responsible for light emission. Both UV- and X-irradiated samples showed only a slight increase in thermoluminescence output, each producing two

small peaks near 100℃ and 200 ℃; the intensities of these peaks increased slightly with irradiation time. These observations support previous claims that CFR-PEEK is more radiation resistant than unfilled PEEK [37].

4.1.3 TSL in HT-PEEK

HT-PEEK shows three TSL peaks at about 100ºC, 200ºC, and 330ºC as in Figure 4-13. The peak at 100ºC is much more affected by X- and UV-irradiation. Its intensity increases with irradiation. Also it was observed that, intensity of peak at 100ºC was greater for 1 hour UV-irradiated sample than 1 hour X-irradiated sample.

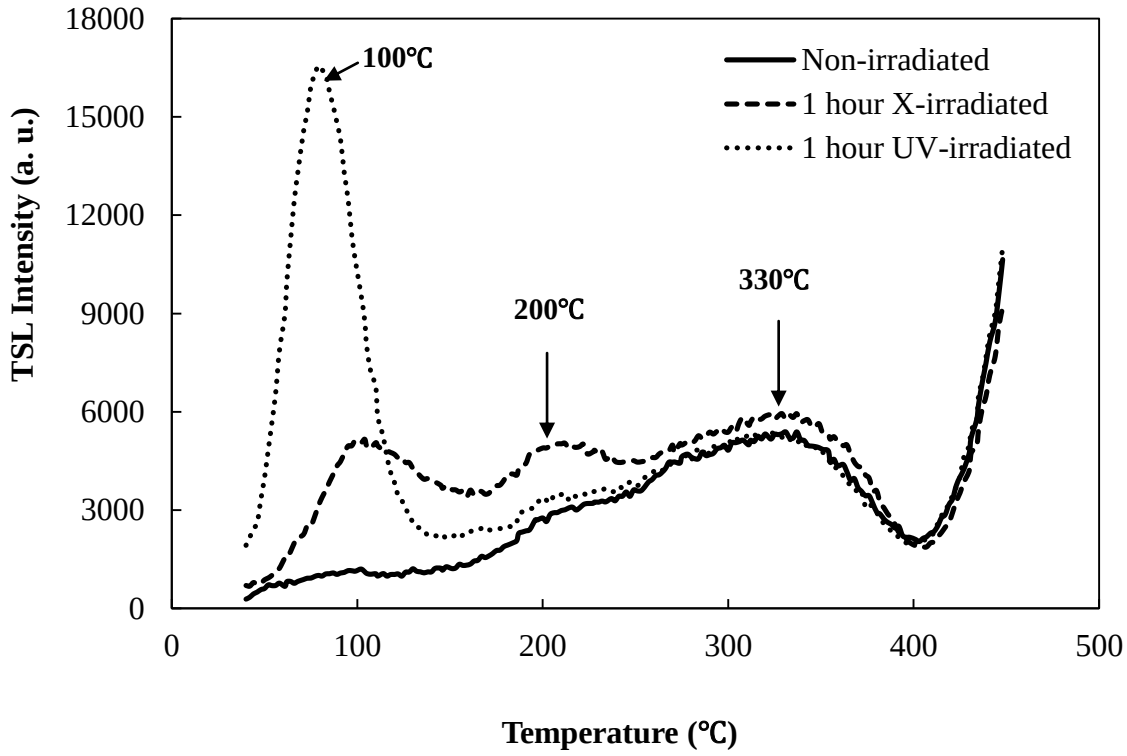

Figure 4-13. TSL of High-Temperature PEEK (HT-PEEK)

4.1.4 TSL in unfilled PEEK (rod)

As seen in Figure 4-15, the TSL glow curve contains 3 major peaks at about 100ºC, 200ºC, and 380ºC for HT-PEEK. The peaks at 100ºC and 200ºC are more affected by X- and UV-irradiation. Also the intensity of these peaks is greater for X-irradiated samples than UV-irradiated samples.

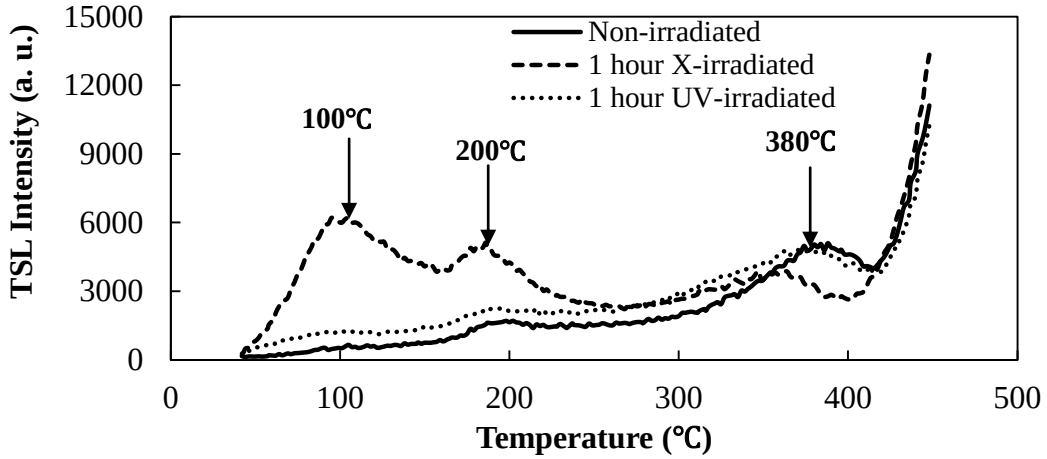

Figure 4-14. TSL of plain PEEK (rod)

4.1.5 TSL of preheated samples

In order to understand the properties of PEEK in more detail, the samples were heated (in oven) before TSL measurements at different temperatures for 1 hour in air. The glow curves for PEEK film (figure 4-16) shows that the intensity of peak 4 (at 150℃) decreases as preheat temperature is increased, and is completely eliminated when the sample is preheated at 250℃ or above. This indicates that the species responsible for TSL were quenched or annealed. A new peak at 75℃ of the glow curve seems to be activated when the samples are preheated, which increases with increases of preheat temperature (see Figure 4-15).

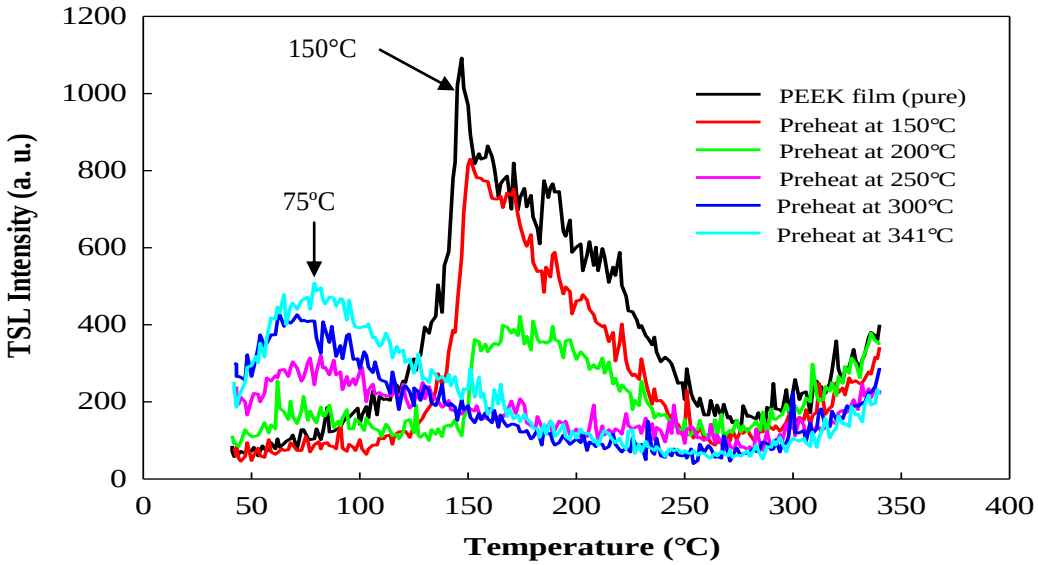

Figure 4-15. Glow curves for preheated PEEK film.

TSL measurement of PEEK film samples at different elapsed time after the sample is preheated at 250°C in air for 1 hour is shown in Figure 4-16.

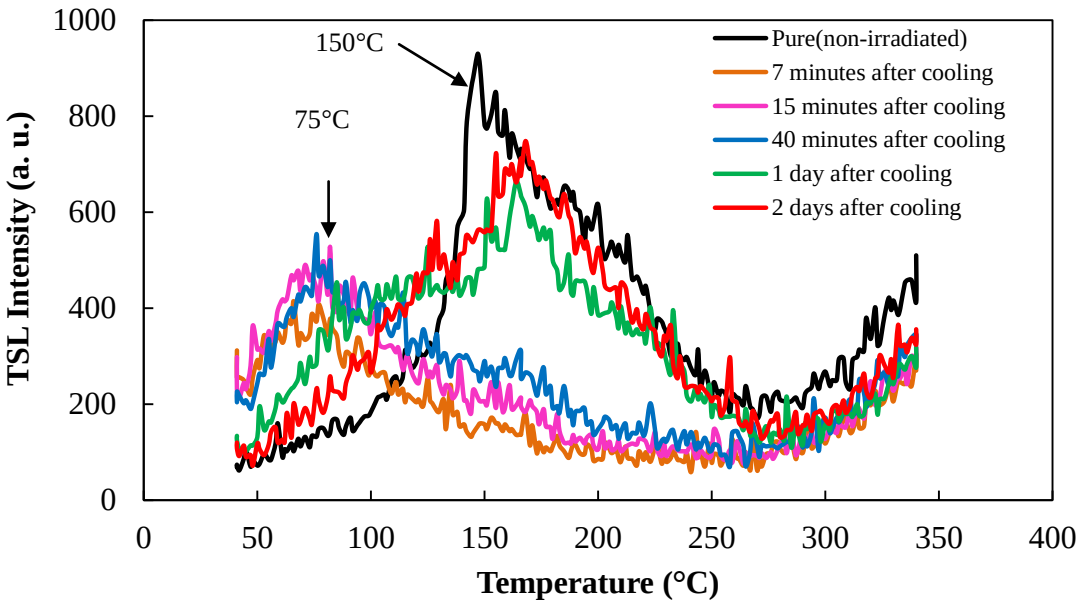

Figure 4-16. Glows curves for 1 hour preheated samples of PEEK film at 250°C in air.

It was observed that the peak at 75°C decreases and the peak at 150°C start to reappear slowly with time when the samples are stored at room temperature in air after preheating. After 2 days, 150°C peak is clearly distinguished (as in pure sample) in the TSL glow curve as in Figure 4-16. The deconvoluted glow curves for preheated samples are shown in Figure 4-17.

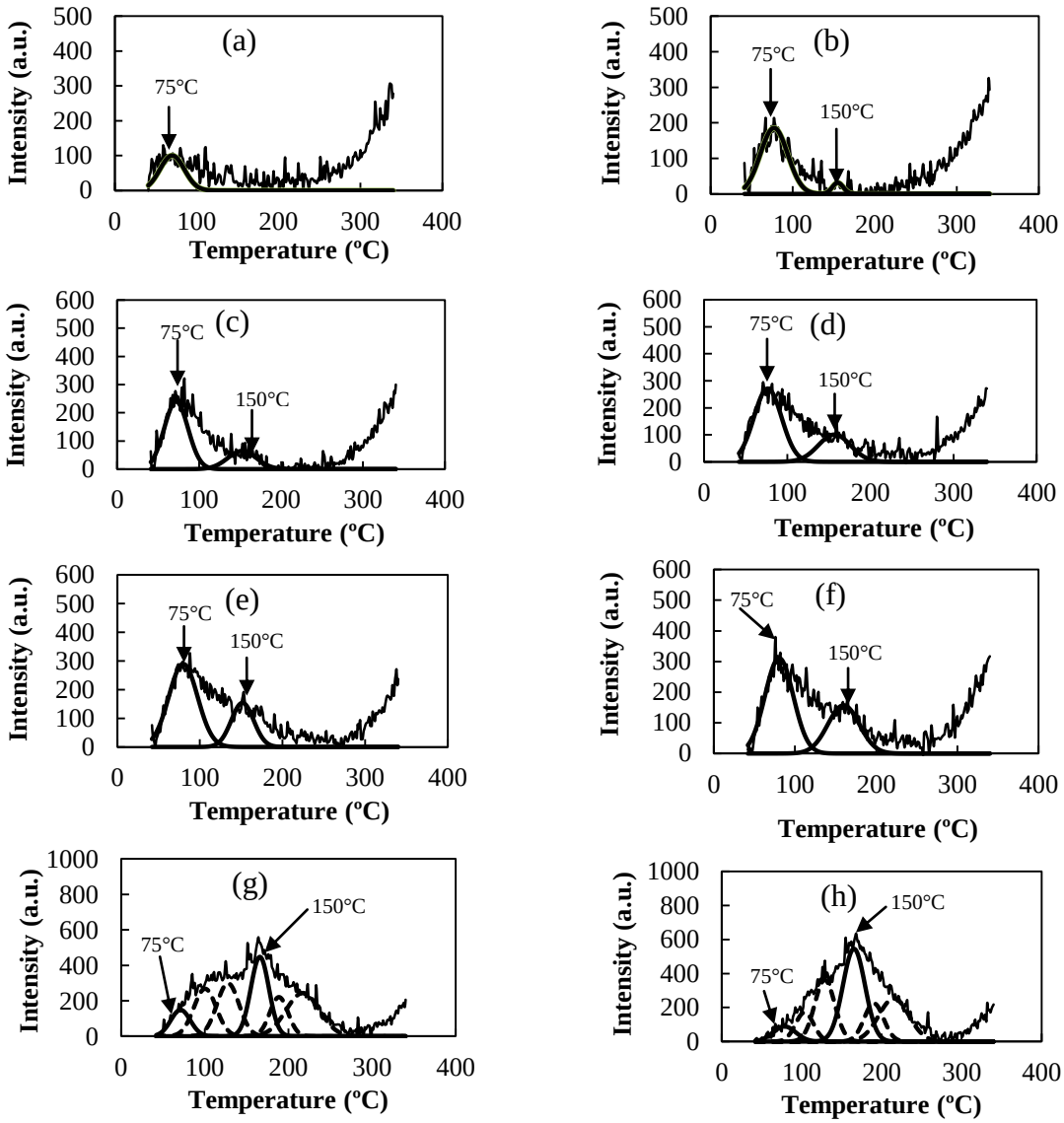

Figure 4-17. (a) Immediately after cooling; (b) 7 minutes after cooling; (c) 15 minutes after cooling; (d) 25 minutes after cooling; (e) 33 minutes after cooling; (f) 40 minutes after cooling; (g) 1 day after cooling; (h) 2 days after cooling.

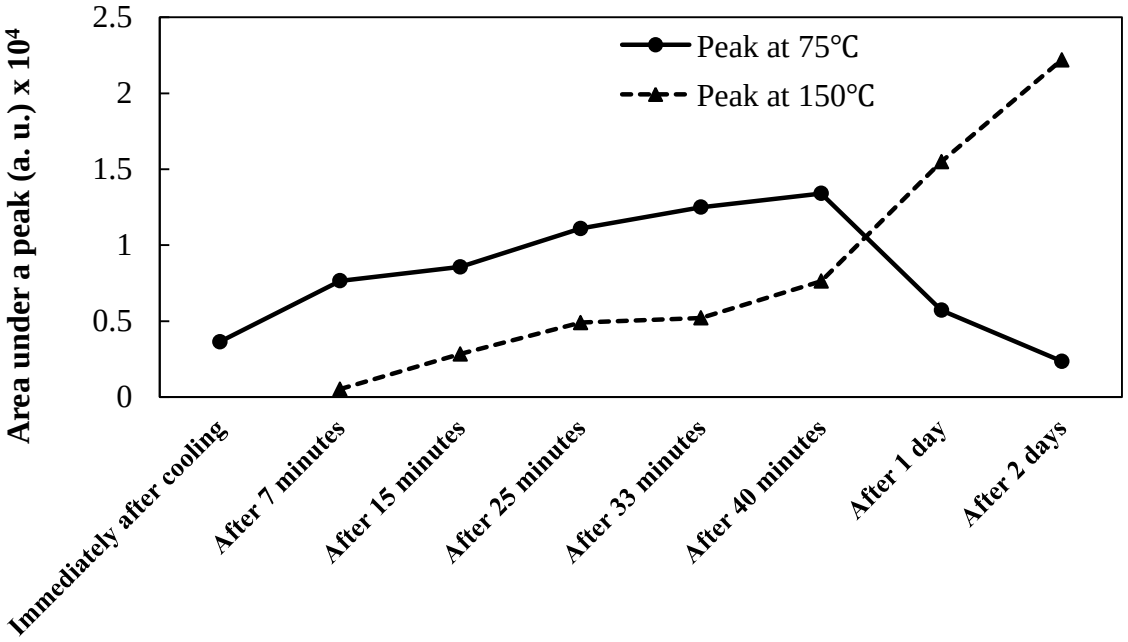

Figure 4-18. Line graph showing decay of peak-2 and growth of peak-4 after preheating PEEK film at 250°C in air for 1 hour.

Samples of CFR-PEEK, HT-PEEK and unfilled PEEK rod were also preheated for 1 hour at different temperatures in air. The results obtained are shown in Figure 4-19, 4-20, and 4-21 respectively.

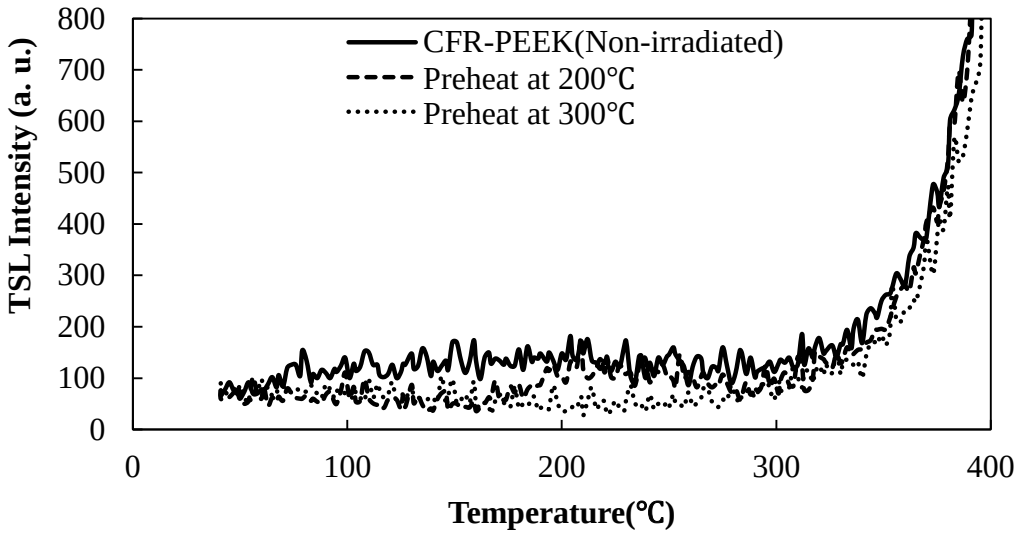

Figure 4-19. TSL glow curves for preheated CFR-PEEK.

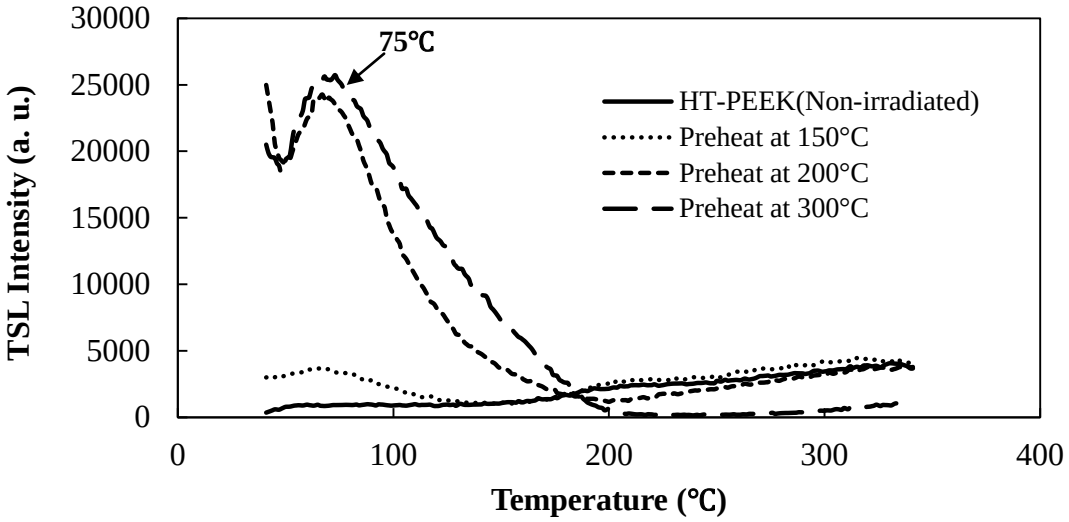

Figure 4-20. TSL glow curves for preheated sample of HT-PEEK.

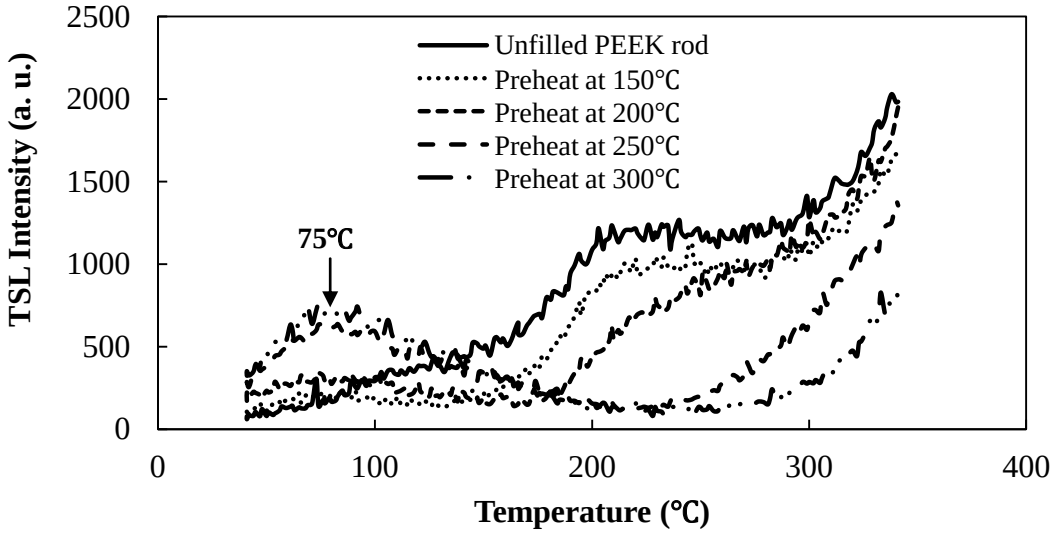

Figure 4-21. TSL glow curves for preheated sample of Unfilled PEEK (rod).

Except for CFR-PEEK, we have clearly observed that a peak at 75ºC seems to appear and its intensity increases with increase of preheat temperature. For CFR-PEEK, we do not observe significant change in the shape of TSL glow curve upon preheats. This may indicate that CFR-PEEK shows a higher thermal stability than the other PEEK grades [28].

4.2 DSC measurement

4.2.1 DSC of X-irradiated PEEK

The DSC heating curves for PEEK film was performed before and after X-irradiation (not UV). Glass transition temperature (T_g), crystallization temperature (T_c), and melting temperature (T_m), were obtained from DSC measurement. The observed values of T_g, T_c, and T_m are given in the Table 4-1. There was a large exothermic crystallization peak T_c~180℃ for PEEK-film which indicates that the material has a strong tendency to crystallize, similar to a study by Li et al. [18]. The 180°C exothermic peak was not observed in CRF-PEEK (figure 4-23), and HT-PEEK (Figure 4-24). This suggests that PEEK film is less crystalline than other PEEKs.

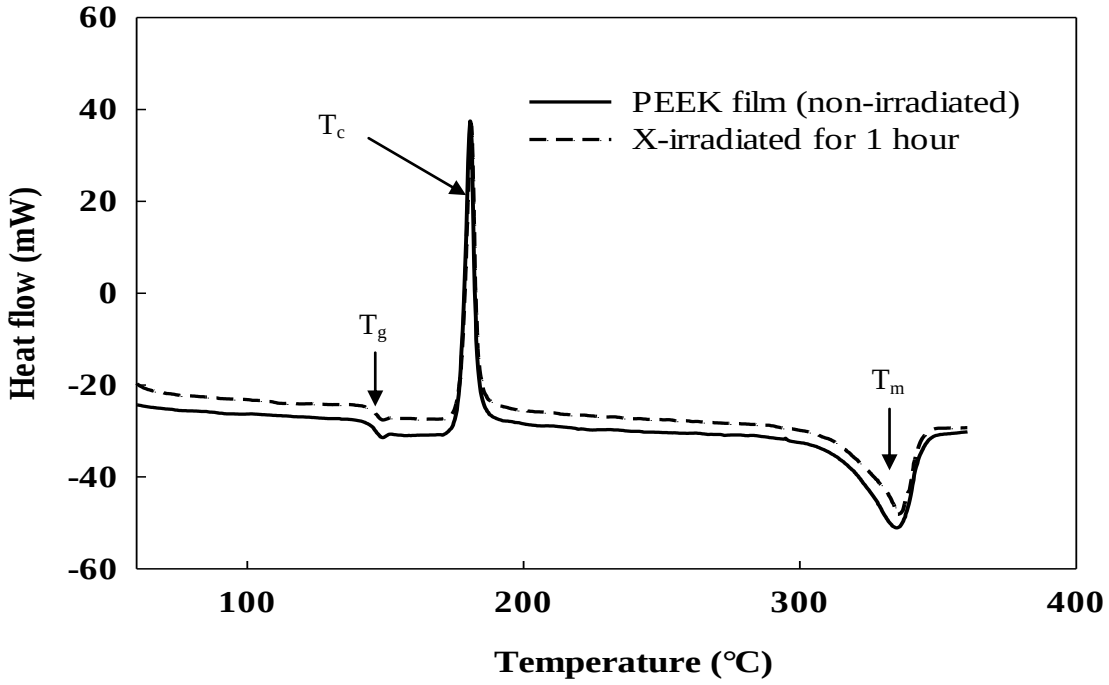

Figure 4-22. DSC curves of PEEK film.

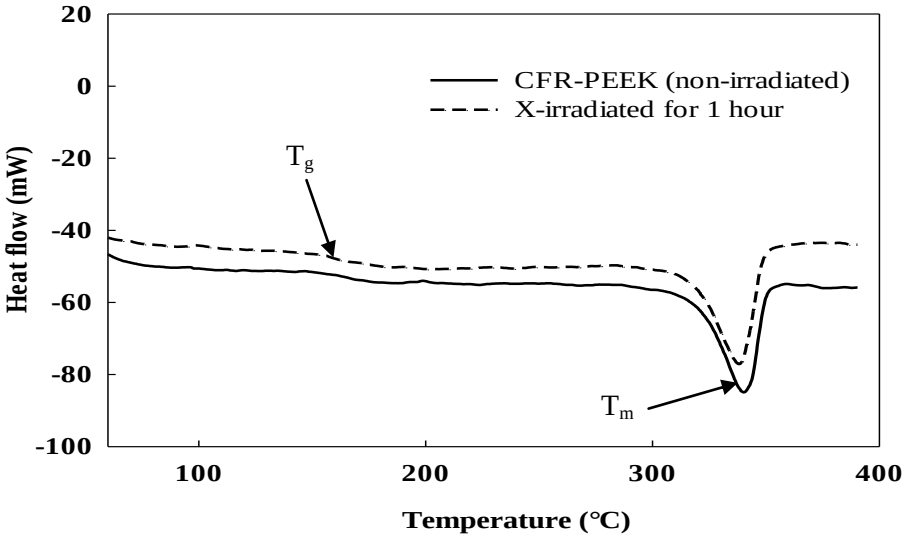

Figure 4-23. DSC curves of CFR-PEEK

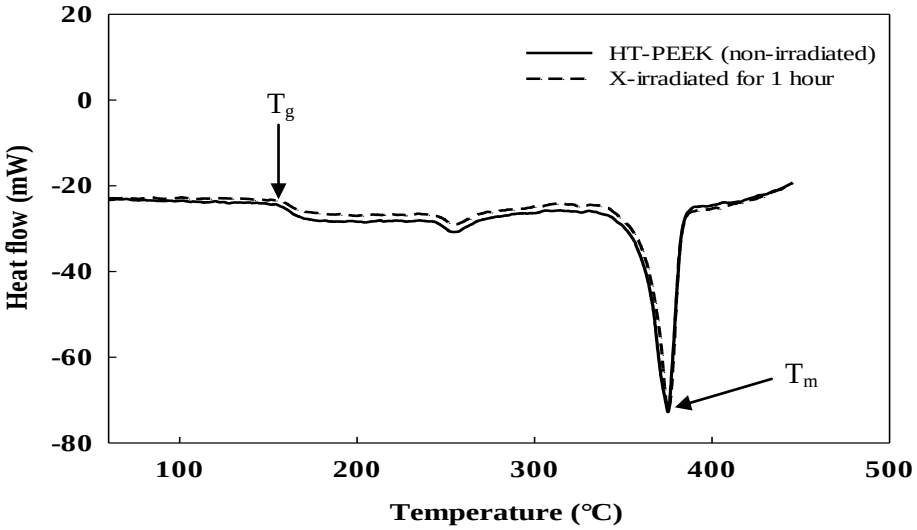

Figure 4-24. DSC curves of HT-PEEK

It was possible to obtain the glass transition temperature (T_g), crystallization temperature (T_c), and melting temperature (T_m) of the different PEEK grades by DSC measurements. The peak indicating the melting temperature appears at about 335°C-340℃ for PEEK-film and CRF-PEEK. HT-PEEK shows a higher melting point at about 374℃.

Table 4-1: Observed values of T_g, T_c,and T_m for different PEEK.

A) For PEEK Film

Samples	**T_g (°C)**	**T_c (°C)**	**T_m (°C)**
PEEK film (pure)	140.50	180.69	335.18
1 hr. X-irradiated (film)	141.06	180.81	334.69

B) For CFR-PEEK

Samples	**T_g (°C)**	**T_m (°C)**
CFR-PEEK	150.68	340.13
1 hr. X-irradiated	152.68	338.06

C) For HT-PEEK

Samples	**T_g (°C)**	**T_m (°C)**
HT-PEEK	143.31	374.25
1 hr. X-irradiated	146.37	374.06

It was observed that the glass transition temperature increases and melting temperature decreases slightly as a result of X-irradiation for all types of PEEK. Similar observations were made by past researchers [18, 23, 43] for PEEK for γ- and e-beam irradiation. Increased cross-linking result reduced mobility of polymer molecule would be expected to increase T_g, T_c, and T_m. However, if chain scission had occurred, the shorter length of polymer molecule would be expected to reduce T_g, T_c, and T_m [18, 43]. The shifting of T_g to higher temperature and T_m to lower temperature with irradiation suggest that crosslinking as well as chain scission mechanism takes place due to X-irradiation.

4.2.2 DSC of preheated samples of PEEK film

DSC heating curves for preheated samples of PEEK film at 250°C for 1 hour in air after different elapsed time after heating is shown in Figure 4-25 (a). The observed values of Tg, Tc and Tm are shon in Table 4-2. Figure 4-25 (b) shows heating curves for pristine sample of PEEK film for first and second DSC run.

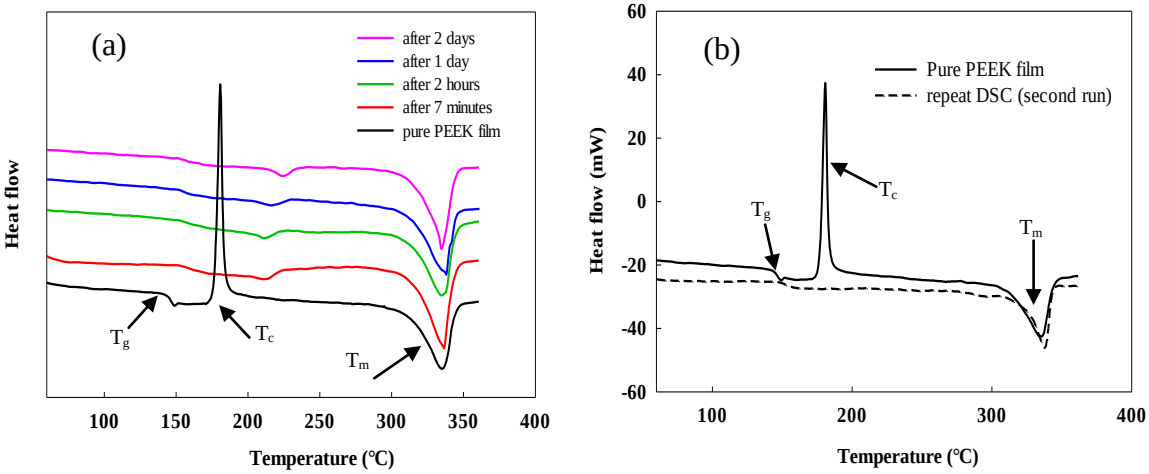

Figure 4-25. (a) DSC curves of preheated PEEK film, (b) DSC curves of PEEK film for first and second run.

Table 4-2: Values of Tg, Tc, and Tm for PEEK film preheated at 250°C in air for 1 hour.

Samples	**T_g (°C)**	**T_c (°C)**	**T_m (°C)**
PEEK film (pure)	140.50	180.69	335.18
After 7 minutes	149.19	-	336.44
After 2 hours	148.13	-	332.38
After 1 day	151.50	-	338.00
After 2 days	148.50	-	334.50

When the PEEK film is preheated at 250°C in air for 1 hour, then the intense exothermic peak present in pristine sample was absent. This may indicates that amount of crystallinity in PEEK film increases once the sample is heated and then cooled. The DSC curves of preheated sample exhibits two melting processes: showing lower temperature

endothermic peak at about 220°C (represents the onset of melting of crystalline regions), and major endothermic peak about 336°C [44]. Similar nature of DSC traces was observed by Vaughan et al. [23] for preheated samples of amorphous PEEK. The lower temperature endothermic peak shifts to higher temperature as we waited for longer time after heating. It was also observed that the heat treatment shift T_g to higher temperature, indicating crosslinking occurs among the molecules of PEEK.

4.3 Conclusion and future work

In this work, we have studied the thermally stimulated luminescence (TSL) and differential scanning calorimetry (DSC) in different grades of PEEK. Results showed that PEEK-film contains a major peak about 150℃, which corresponds to the glass transition temperature of PEEK. Minor glow peaks at 75°C, 100°C, 124°C, 180°C and 210°C were resolved using TSL deconvolution program. Thermal activation energy associated with these glow peaks ranges between 0.89 eV and 3.2 eV, and the reaction mechanism seem to follow a kinetic order of 1.5. The peak at 100°C was activated by irradiation and its intensity increases with dose for both UV and X-irradiation.

It was observed that the glass transition temperature increases and melting temperature decreases slightly as a result of X-irradiation for all types of PEEK. This suggests that both crosslinking as well as chain scission mechanism takes place due to X-irradiation. For CFR-PEEK, there were no significant changes caused by radiation (UV- and X-ray), indicating it is more radiation resistant than the other grades of PEEK studied in this work.

For future, it is recommended to correlate the ESR and TSL, and DSC study to better investigate the effect of irradiation on PEEK polymer.

References

1. M. P. Stevens, Polymer Chemistry, 3rd edition, Oxford University Press, 1999.

2. L. S. Nair and C. T. Laurencin, Polymers as biomaterials for tissue engineering and controlled drug delivery, Adv. Biochem Engin/Biotechnol, 102 (2006) 47-90

3. F. W. Billmeyer, Text book of polymer science, John Wiley and Sons, Inc., 1971

4. G. Natta, P. Pino, P. Corradini, F. Danusso, E. Mantica, G. Mazzanti and G. Moraglio, J. Am. Chem. Soc., 77 (1955) 1708-1710

5. D. F. Williams, The Williams dictionary of biomaterials. Liverpool University Press, Liverpool, 1999

6. R. Barbucci (ed), Integrated biomaterial science, Kluwer/Plenum, New York, 2002

7. R. Huiskes, Some fundamental aspects of human-joint replacement, Acta Orthop Scand, Acta Orthop Scand Suppl., 1980

8. S. Ramkrishna, J. Mayer, E. Wintermantel and K. W. Leong, Biomedical applications of polymer-composite materials, Composites science and Technology, 61 (2001) 1189-1224

9. S. Green and J. Schlegel, A polyaryletherketone biomaterials for use in medical implants applications, Proceedings of a conference held in Brussels, 2001.

10. K. J. L. Burg and S. W. Shalaby, PES and PEEK, Encyclopedia of materials: Science and Technology, (2001) 6837-6839

11. S. Thomas and Vikash P. M, Hand book of engineering and speciality thermoplastics, polyethers and polyesters, Scrivener publishing, Vol. 3, 2011

12. S. M. Kurtz and J. N. Devine, PEEK biomaterials in trauma, Orthopedic and spinal implants, 28 (2007) 4845-4869

13. P. C. Dawson and D. J. Blundell, x-ray data for poly (aryl ether ketones) polymer, 21 (1980) 577-578

14. S. M. Kurtz, PEEK biomaterials handbook, 1st edition, Elsevier Inc., 2012

15. ZEUS, Technical whitepaper focus on PEEK, Zeus industrial products, Inc., 2005

16. M. S. Jahan, C. Wang, G. Schwartz and J. A. Davidson, Combined chemical and mechanical effects on free radicals on UHMWPE joints during implantation, J. Biomat. Mater. Res, 25 (1991) 1005

17. M. S. Jahan, D. E. Thomas, K. Banerjee, H. H. Trieu, W. O. Haggard and J. E. Parr, Effects of radiation-sterilization on medical implants, Radiat. Phys. Chem., 51 (1998) 593-594

18. H. M. Li, R. A. Fouracre, M. J. Given, H. M. Banford, S. Wysocki, and S. Karolczak, The Effect on polyetheretherketone and polyethersulfone of electron and γ irradiation, IEEE transactions on dielectrics and electrical insulation, 6 (1999) 295-302

19. E. S. A. Hegazy, T. Sasuga, M. Nishii and T. Seguchi, Irradiation effects on aromatic polymers, J. Polymer, 33 (1992) 2897-2910

20. T. Sasuga and M. Hagiwara, Molecular motions of non-crystalline poly (aryl ether ether ketone) PEEK and influence of electron beam irradiation, J. Polymer, 26 (1985) 501-505

21. O. Yoda and I. Kuriyama, Crystallite size distribution and the lattice distortions in highly γ-irradiated linear polyethylene, J. of Material Science, 14 (1979) 1733-1743.

22. A. S. Vaughan and S. J. Sutton, On radiation effects in oriented poly (ether ether ketone), Polymer, 36 (1995) 1549-1554

23. A. S. Vaughan and G. C. Stevens, On crystallization, morphology and radiation effects in poly (ether ether ketone), 36 (1995) 1531-1547

24. E. Richaud, P. Ferreira, L. Audouin, X. Colin, J. Verdu and C. M. Leroy, Radiochemical aging of poly(ether ether ketone), European Polymer Journal, 46 (2010) 731-743

25. P. D. Sahare, R. S. Porter and S. V. Moharil, High-temperature thermoluminescence in poly (etherether ketone) fibers, Journal of materials science letters, 11 (1992) 822-823

26. S. K. Brauman and J. G. Pronko, Chemiluminescence studies of the thermo oxidation of PEEK, Journal of Polymer Science Part B: Polymer Physics, 26 (1988) 1205-1216

27. G. Zhang, C. Zhang, P. Nardin, W. Y. Li, H. Liao, and C. Coddet, Effects of sliding velocity and applied load on the tribological mechanism of amorphous poly-ether-ether-ketone (PEEK), "Tribology International, 41 (2008) 79-86

28. D. J. Kemmish and J. N. Hay, The effect of physical ageing on the properties of amorphous PEEK, Polymer, 6 (1985) 905-912

29. J. R. Atkinson, J. N. Hay and M. J. Jenkins, Enthalpic relaxation in semi crystalline PEEK, Polymer, 43 (2002) 731-735

30. J. N. Hay and D. J. Kemmish, Thermal decomposition of poly (aryl ether ether ketones), polymer, 28 (1987) 2047- 2051

31. A. M. Diez-Pascual, M. Naffakh, M. A. Gomez, C. Marco, G. Ellis, M. T. Martinez, A. Anson, J. M. Gonzalez-Dominguez, Y. M. Rubi and B. Simard, Development and characterization of PEEK/Carbon nanotube composites, J. Carbon, 47 (2009) 3079-3090

32. S. Utzschneider, F. Becker, T. M. Grupp, B. Sievers, A. Paulus, O. Gottschalk and V. Jansson, Inflammatory response against different carbon fiber-reinforced PEEK wear particles compared with UHMWPE in vivo, J. Acta Biomaterialia, 6 (2010) 4296-4304

33. M. Sharma, J. Bijwe and P. Mitschang, Wear performance of PEEK-Carbon fabric composites with strengthened fiber-matrix interface, J. wear, 271 (2011) 2261-2268

34. A. Wang, R. Lin, C. Stark and J. H. Dumbleton, Suitability and limitations of Carbon fiber reinforced PEEK composite as bearing surfaces for total joint replacements, J. Wear, Vol. 225-229 (1999) 724-727

35. C. M. Ma, C. Lee and N. Tai, Chemical resistance of Carbon fiber reinforced poly(ether ether ketone) and poly(phenylene sulfide) composites, J. Polymer Composites, 13 (1992) 435-440

36. A. Almajid, K. Friedrich, J. Floeek and T. Burkhart, Surface damage characteristics and specific wear rates of a new continuous CFR-PEEK composite under sliding and rolling contact conditions, Appl. Compos Mater, 18 (2011) 211-230

37. A. Godara, D. Raabe and S. Green, The influence of sterilization processes on the micromechanical properties of Carbon fiber-reinforced PEEK composites for bone implant applications, J. Acta Biomaterialia, 3 (2007) 209-220

38. R. Chen and S. W. S. McKeever, Theory of thermoluminescence and related phenomena, World scientific, Singapore, 1997

39. D. R. Vij, Luminescence of solids, Plenum Press, New York, 1998

40. J. M. Gray, A thermally stimulated luminescence investigation of the oxidation in gamma sterilized UHMWPE, Master's Thesis, The University of Memphis, 2005

41. D. Braun, H. Cherdron, M. Rehahn, H. Ritter and B. Voit, polymer synthesis: Theory and practice, 4th edition, springer, 2005

42. T. Sasuga and M. Hagiwara, Radiation deterioration of several aromatic polymers under oxidative conditions, J. Polymer, 28 (1987) 1915-1921

43. T. Sasuga and M. Hagiwara, Mechanical relaxation of crystalline poly (aryl ether ether ketone) PEEK and influence of electron beam irradiation, J. Polymer, 27 (1986) 821-826

44. O. Yoda, The radiation effect on non-crystalline poly(aryl-ether-ketone) as revealed by x-ray diffraction and thermal analysis, Polymer communications, 28 (1984) 238-240

Appendix

Glow curve parameters for PEEK (film)

Table A-1: Non-irradiated PEEK film

Peak	T_{max}(℃)	τ(℃)	δ(℃)	μ_g	K. order(I)	E(eV)	S(s^{-1})
1	72	16.4	15.7	0.489	1.561	0.969	1.20E+13
2	101	15.2	13.5	0.47	1.371	1.209	1.74E+15
3	123	12.4	11.5	0.481	1.478	1.708	6.45E+20
4	152	14.4	13.2	0.478	1.448	1.68	8.52E+18
5	181	19.6	18.8	0.49	1.566	1.413	3.46E+14
6	209	30.2	28.3	0.484	1.504	0.99	8.81E+08

Table A-2: PEEK film X-irradiated for 10 minutes

a) Immediately after irradiation

Peak	T_{max}(℃)	τ(℃)	δ(℃)	μ_g	K. order(I)	E (eV)	S(s^{-1})
1	63	14.3	13.1	0.478	1.447	1.047	4.81E+14
2	86	19.4	18.9	0.493	1.609	0.887	1.85E+11
3	120	18.5	17.9	0.492	1.59	1.118	1.64E+13
4	149	8.7	7.8	0.473	1.394	2.774	2.19E+32
5	169	13.4	12	0.472	1.391	1.947	1.70E+21
6	208	24.7	23.5	0.488	1.544	1.243	5.65E+11

b) 15 minutes after irradiation

Peak	T_{max}(℃)	τ(℃)	δ(℃)	μ_g	K. order(I)	E(eV)	S(s^{-1})
1	77	16.6	15.7	0.486	1.528	0.982	1.12E+13
2	100	15.8	14.4	0.477	1.434	1.165	4.72E+14
3	125	15.3	14.3	0.483	1.497	1.391	3.69E+16
4	148	7.8	6.6	0.458	1.262	3.012	2.24E+35
5	167	12.8	11.9	0.482	1.484	2.056	3.75E+22
6	203	22.4	21.7	0.492	1.593	1.357	1.42E+13

c) 25 minutes after irradiation

Peak	T_{max}(℃)	τ(℃)	δ(℃)	μ_g	K. order(I)	E(eV)	S(s^{-1})
1	77	15.5	14.7	0.487	1.536	1.058	1.50E+14
2	101	13.3	12.6	0.486	1.533	1.418	1.46E+18
3	126	15	13.5	0.474	1.403	1.404	5.20E+16
4	148	7.5	5.9	0.44	1.114	3.033	4.01E+35
5	170	16.2	15.4	0.487	1.542	1.64	3.88E+17
6	206	24.2	22.5	0.482	1.484	1.253	8.03E+11

d) 48 hours after irradiation

Peak	T_{max}(℃)	τ(℃)	δ(℃)	μ_g	K. order(I)	E(eV)	S(s^{-1})
1	70	13.4	12.7	0.487	1.534	1.181	2.39E+16
2	101	13.9	13.1	0.485	1.519	1.355	1.89E+17
3	126	14.4	13.5	0.484	1.505	1.492	6.71E+17
4	147	9.8	8.4	0.462	1.29	2.387	6.38E+27
5	168	14.9	13.3	0.472	1.383	1.735	6.22E+18
6	204	27.7	25.7	0.481	1.479	1.073	9.68E+09

Table A-3: PEEK film X-irradiated for 20 minutes

a) Immediately after irradiation

Peak	T_{max}(℃)	τ(℃)	δ(℃)	μ_g	K.order(I)	E(eV)	S(s^{-1})
1	69	16	14.7	0.479	1.454	0.966	1.41E+13
2	95	18.5	17.8	0.49	1.574	0.979	1.78E+12
3	124	16.1	14.3	0.47	1.371	1.286	1.08E+15
4	149	8	7	0.467	1.337	2.989	9.75E+34
5	165	17	15.4	0.475	1.419	1.501	1.44E+16
6	204	27.9	26.4	0.486	1.53	1.071	9.40E+09

b) 15 minutes after irradiation

Peak	T_{max}(℃)	τ(℃)	δ(℃)	μ_g	K. order(I)	E(eV)	S(s^{-1})
1	80	15.4	14.4	0.483	1.499	1.079	2.24E+14
2	104	16.8	15.6	0.481	1.481	1.123	8.32E+13
3	403	15.5	14.5	0.483	1.5	1.407	3.54E+16
4	130	7.8	7.1	0.477	1.431	3.058	5.70E+35
5	168	11.3	10	0.467	1.339	2.295	2.13E+25
6	205	28.9	28.3	0.495	1.623	1.047	4.72E+09

c) 25 minutes after irradiation

Peak	T_{max}(℃)	τ(℃)	δ(℃)	μ_g	K. order(I)	E(eV)	S(s^{-1})
1	78	16.2	14.6	0.474	1.406	0.999	1.77E+13
2	103	16.9	15.4	0.477	1.433	1.105	5.03E+13
3	131	15.9	14.5	0.477	1.435	1.364	9.02E+15
4	152	7.8	6.8	0.466	1.328	3.115	1.57E+36
5	171	10.8	9.9	0.478	1.448	2.48	1.91E+27
6	204	27.1	26.5	0.494	1.619	1.118	3.02E+10

d) 1 hour after irradiation

Peak	T_{max}(℃)	τ(℃)	δ(℃)	μ_g	K. order(I)	E(eV)	S(s^{-1})
1	78	18.1	16.7	0.48	1.464	0.896	5.17E+11
2	101	14.4	13.6	0.486	1.525	1.309	4.21E+16
3	126	14.2	13.3	0.484	1.503	1.514	1.27E+18
4	149	9.3	8.5	0.478	1.441	2.602	1.99E+30
5	170	12.4	11.3	0.477	1.433	2.134	2.22E+23
6	207	26.8	25.4	0.487	1.534	1.135	3.86E+10

Table A-4: PEEK film X-irradiated for 30 minutes

a) Immediately after irradiation

Peak	T_{max}(℃)	τ(℃)	δ(℃)	μ_g	K. order(I)	E(eV)	S(s^{-1})
1	72	16.1	14.9	0.481	1.472	0.977	1.59E+13
2	97	18.9	17.7	0.484	1.503	0.959	7.74E+11
3	126	15.6	14.5	0.482	1.483	1.367	1.61E+16
4	149	6.5	5.9	0.44	1.114	3.047	4.91E+35
5	166	14.5	13.2	0.477	1.431	1.782	2.75E+19
6	199	29.8	29.3	0.496	1.634	0.989	1.48E+09

b) 15 minutes after irradiation

Peak	T_{max}(℃)	τ(℃)	δ(℃)	μ_g	K.order(I)	E(eV)	S(s^{-1})
1	74	14.5	13.8	0.488	1.545	1.117	1.57E+15
2	100	18.7	17.4	0.482	1.486	0.985	1.36E+12
3	126	11.8	10.9	0.48	1.467	1.824	1.35E+22
4	147	9.3	8.4	0.475	1.412	2.572	1.13E+30
5	168	12.1	10.5	0.465	1.318	2.129	2.53E+23
6	203	27.8	26.8	0.491	1.58	1.077	1.16E+10

c) 51 minutes after irradiation

Peak	T_{max}(℃)	τ(℃)	δ(℃)	μ_g	K. order(I)	E(eV)	S(s^{-1})
1	75	13.9	13.1	0.485	1.519	1.168	8.56E+15
2	103	20.4	19.8	0.493	1.598	0.923	1.50E+11
3	130	13.5	12.6	0.483	1.494	1.627	2.28E+19
4	151	8	7	0.467	1.337	3.025	1.61E+35
5	169	10.5	9.7	0.48	1.468	2.537	1.16E+28
6	207	28.9	28.4	0.496	1.633	1.054	5.29E+09

d) 1 hour after irradiation

Peak	T_{max}(℃)	τ(℃)	δ(℃)	μ_g	K. order(I)	E(eV)	S(s^{-1})
1	80	16.6	15.7	0.486	1.528	0.999	1.51E+13
2	101	18.6	17.7	0.488	1.545	0.998	2.10E+12
3	126	15.5	14.3	0.48	1.464	1.372	1.91E+16
4	150	6.9	6.8	0.459	1.272	2.969	4.52E+34
5	168	11.9	11.2	0.485	1.516	2.232	3.95E+24
6	195	31.5	31.3	0.498	1.665	0.917	2.86E+08

Table A-5: PEEK film X-irradiated for 40 minutes

a) Immediately after irradiation

Peak	T_{max}(℃)	τ(℃)	δ(℃)	μ_g	K. order(I)	E(eV)	S(s^{-1})
1	74	15.6	14.6	0.483	1.501	1.027	7.20E+13
2	101	19.5	18.8	0.491	1.58	0.957	5.22E+11
3	127	12.7	11.6	0.477	1.439	1.696	2.52E+20
4	148	8.4	7.8	0.481	1.481	2.89	7.46E+33
5	170	12	11.2	0.483	1.494	2.222	2.46E+24
6	202	26.2	25	0.488	1.552	1.137	5.79E+10

b) 15 minutes after irradiation

Peak	T_{max}(℃)	τ(℃)	δ(℃)	μ_g	K.order(I)	E(eV)	S(s^{-1})
1	76	14.1	13	0.48	1.463	1.148	3,87E15
2	100	15.4	14.5	0.485	1.517	1.212	2.10E+15
3	124	12.8	12.2	0.488	1.549	1.68	2.27E+20
4	149	9.9	9.3	0.484	1.511	2.461	3.95E+28
5	170	13.5	12.3	0.477	1.433	1.957	1.88E+21
6	205	24.3	23.6	0.493	1.6	1.257	9.83E+11

c) 30 minutes after irradiation

Peak	T_{max}(℃)	τ(℃)	δ(℃)	μ_g	K.order(I)	E(eV)	S(s^{-1})
1	75	14.3	13.7	0.489	1.563	1.139	3.17E+15
2	101	18.6	17.9	0.49	1.575	1.002	2.36E+12
3	127	13.5	11.6	0.462	1.295	1.553	3.66E+18
4	150	9	8.3	0.48	1.463	2.712	3.62E+31
5	171	12.9	11.4	0.469	1.36	2.034	1.37E+22
6	204	26.2	25	0.488	1.552	1.147	6.57E+10

d) 1 hour after irradiation

Peak	T_{max}(℃)	τ(℃)	δ(℃)	μ_g	K.order(I)	E(eV)	S(s^{-1})
1	78	14.6	13.8	0.486	1.527	1.133	1.72E+15
2	103	16.2	15.6	0.491	1.577	1.175	4.78E+14
3	127	15.1	13.4	0.47	1.369	1.398	3.67E+16
4	154	10.7	9.9	0.481	1.472	2.315	3.09E+26
5	174	12.1	11.3	0.483	1.495	2.249	2.76E+24
6	205	31.9	31.5	0.497	1.647	0.943	3.35E+08

Table A-6: PEEK film X-irradiated for 50 minutes

a) Immediately after irradiation

Peak	T_{max}(℃)	τ(℃)	δ(℃)	μ_g	K.order(I)	E(eV)	S(s^{-1})
1	73	15.6	15	0.49	1.573	1.030	8.83E+13
2	99	19.8	18.6	0.484	1.511	0.921	1.98E+11
3	127	14.8	14.1	0.488	1.548	1.464	2.63E+17
4	147	7.9	7	0.455	1.234	2.943	3.94E+34
5	167	12.1	11.3	0.483	1.495	2.173	1.00E+24
6	203	26.2	25	0.488	1.552	1.142	6.17E+10

b) 15 minutes after irradiation

Peak	T_{max}(℃)	τ(℃)	δ(℃)	μ_g	K.order(I)	E(eV)	S(s^{-1})
1	73	13.6	13	0.489	1.557	1.190	2.17E+16
2	100	17.4	16.7	0.49	1.568	1.072	2.33E+13
3	124	12.4	11.6	0.483	1.500	1.727	9.12E+20
4	148	8.3	7.5	0.475	1.413	2.900	9.74E+33
5	169	12	11.2	0.483	1.494	2.212	2.15E+24
6	194	30.6	29.7	0.493	1.598	0.936	4.97E+08

c) 45 minutes after irradiation

Peak	T_{max}(℃)	τ(℃)	δ(℃)	μ_g	K.order(I)	E(eV)	S(s^{-1})
1	78	15.5	14.6	0.485	1.518	1.065	1.63E+14
2	104	17.5	16.6	0.487	1.536	1.082	2.32E+13
3	127	12.4	11.6	0.483	1.5	1.753	1.36E+21
4	150	8.3	7.5	0.475	1.413	2.935	1.59E+34
5	171	13.1	12.2	0.482	1.488	2.045	1.72E+22
6	208	27.9	26.8	0.49	1.57	1.096	1.37E+10

d) 24 hours after irradiation

Peak	T_{max}(℃)	τ(℃)	δ(℃)	μ_g	K.order(I)	E(eV)	S(s^{-1})
1	80	14.4	13.8	0.489	1.564	1.168	4.50E+15
2	102	12.9	12.1	0.484	1.507	1.476	7.16E+18
3	125	14	12.5	0.472	1.384	1.499	9.72E+17
4	149	9.9	9	0.476	1.428	2.434	1.84E+28
5	170	14.7	13.2	0.473	1.398	1.781	1.71E+19
6	204	28.9	28.4	0.496	1.633	1.043	4.58E+09

Table A-7: PEEK film X-irradiated for 60 minutes

a) Immediately after irradiation

Peak	T_{max}(℃)	τ(℃)	δ(℃)	μ_g	K.order(I)	E(eV)	S(s^{-1})
1	73	15.9	14.7	0.48	1.47	0.996	2.78E+13
2	99	20.4	19.8	0.493	1.598	0.901	1.04E+11
3	128	15.3	14.5	0.487	1.534	1.419	6.17E+16
4	148	7.7	7.1	0.48	1.463	3.154	1.16E+37
5	168	15	14.2	0.486	1.531	1.76	1.20E+19
6	203	24.5	23.5	0.49	1.566	1.231	5.80E+11

b) 15 minutes after irradiation

Peak	T_{max}(℃)	τ(℃)	δ(℃)	μ_g	K.order(I)	E(eV)	S(s^{-1})
1	77	15.4	14.7	0.488	1.553	1.067	2.07E+14
2	103	17.5	16.6	0.487	1.536	1.076	2.11E+13
3	126	13	12.3	0.486	1.529	1.666	1.17E+20
4	150	8.4	7.6	0.475	1.416	2.893	5.53E+33
5	169	13.1	12.3	0.484	1.509	2.032	1.56E+22
6	202	29.8	29.3	0.496	1.634	1	1.71E+09

c) 33 minutes after irradiation

Peak	T_{max}(℃)	τ(℃)	δ(℃)	μ_g	K.order(I)	E(eV)	S(s^{-1})
1	75	13.5	12.8	0.487	1.535	1.211	3.50E+16
2	101	16.4	15.7	0.489	1.561	1.145	2.26E+14
3	124	11.5	10.8	0.484	1.51	1.866	6.11E+22
4	147	7.9	7.3	0.48	1.468	3.06	1.03E+36
5	168	16.8	15.9	0.486	1.53	1.562	5.83E+16
6	204	27.8	26.8	0.491	1.58	1.082	1.23E+10

d) 1 hour after irradiation

Peak	T_{max}(℃)	τ(℃)	δ(℃)	μ_g	K. order(I)	E(eV)	S(s^{-1})
1	76	14.5	13.9	0.489	1.564	1.133	2.15E+15
2	104	17.4	16.8	0.491	1.584	1.095	3.46E+13
3	129	12.2	11.5	0.485	1.52	1.806	4.89E+21
4	153	8.4	7.8	0.481	1.481	2.98	1.97E+34
5	170	9.4	8.4	0.472	1.386	2.817	1.84E+31
6	208	30.7	30.3	0.497	1.645	0.994	1.07E+09

e) 24 hours after irradiation

Peak	T_{max}(℃)	τ(℃)	δ(℃)	μ_g	K.order(I)	E(eV)	S(s^{-1})
1	85	15.4	14.8	0.49	1.571	1.12	5.29E+14
2	104	12.4	11.6	0.483	1.5	1.554	6.50E+19
3	125	15.4	14.5	0.485	1.517	1.381	2.86E+16
4	150	7.9	6	0.432	1.049	2.9	1.68E+33
5	169	13.9	13.1	0.485	1.519	1.912	6.32E+20
6	202	31.6	31.3	0.498	1.655	0.942	3.77E+08

Table A-8: Area under a peak for x-irradiated samples of PEEK film immediately after irradiation for different time.

Time of exposure (minute)	Peak 2	Peak 4
0	2.09E+03	1.33E+04
10	8.15E+04	3.51E+04
20	1.25E+05	4.21E+04
30	1.43E+05	4.70E+04
40	2.01E+05	9.19E+04
50	2.15E+05	8.33E+04
60	2.33E+05	8.73E+04

Table A-9: Area under a peak for x-irradiated samples of PEEK film

a) 10 min X-irradiated

Time ellapsed	Peak 2	Peak 4
Immediately	8.15E+04	3.51E+04
After 15 min.	1.79E+04	1.89E+04
After 25 min.	1.60E+04	1.69E+04
After 48 hrs.	7.15E+03	2.12E+04
Non-irradiated	2.09E+03	1.33E+04

b) 20 min X-irradiated

Time ellapsed	Peak 2	Peak 4
Immediately	1.25E+05	4.21E+04
After 15 min.	5.40E+04	3.08E+04
After 25 min.	5.82E+04	3.18E+04
After 1 hr.	2.60E+04	3.43E+04
Non-irradiated	2.09E+03	1.33E+04

c) 30 min X-irradiated

Time ellapsed	Peak 2	Peak 4
Immediately	1.43E+05	4.70E+04
After 15 min.	8.91E+04	5.42E+04
After 51 min.	6.30E+04	3.94E+04
After 1 hour	2.09E+04	2.42E+04
Non-irradiated	2.09E+03	1.33E+04

d) 40 min X-irradiated

Time ellapsed	Peak 2	Peak 4
Immediately	2.01E+05	9.19E+04
After 15 min.	8.90E+04	8.15E+04
After 30 min.	8.28E+04	6.49E+04
After 1 hr	5.09E+04	5.69E+04
Non-irradiated	2.09E+03	1.33E+04

e) 50 min X-irradiated

Time ellapsed	Peak 2	Peak 4
Immediately	2.15E+05	8.33E+04
After 15 min.	1.17E+05	7.41E+04
After 45 min.	6.62E+04	4.93E+04
After 24 hrs.	1.72E+04	3.98E+04
Non-irradiated	2.09E+03	1.33E+04

f) 60 min X-irradiated

Time ellapsed	Peak 2	Peak 4
Immediately	2.33E+05	8.73E+04
After 15 min.	9.82E+04	6.50E+04
After 33 min.	8.18E+04	5.66E+04
After 1 hr.	6.43E+04	5.16E+04
After 24 hrs.	9.26E+03	1.94E+04
Non-irradiated	2.09E+03	1.33E+04

Table A-10: Area under a peak for PEEK film preheated in air for 1 hour at 250°C

Time elapsed	Peak at 75°C	Peak at 150°C
Immediately after cooling	3.64E+03	---
After 7 minutes	7.64E+03	5.24E+02
After 15 minutes	8.57E+03	2.84E+03
After 25 minutes	1.11E+04	4.90E+03
After 33 minutes	1.25E+04	5.21E+03
After 40 minutes	1.34E+04	7.63E+03
After 1 day	5.71E+03	1.55E+04
After 2 days	2.35E+03	2.22E+04